1-5-2016

Influence of hemlock woolly adelgid infestation on the physiological and reflectance characteristics of eastern hemlock

Justin Patrick Williams
University of New Hampshire, Durham

Ryan P. Hanavan
USDA Forest Service

Barrett N. Rock
University of New Hampshire, Durham

Subhash C. Minocha
University of New Hampshire, Durham

Ernst Linder
University of New Hampshire, Durham

Comments

This is a preprint of an article published by Canadian Science Publishing in Canadian Journal of Forest Research in 2016, the Version of Record is available online: https://dx.doi.org/10.1139/cjfr-2015-0328

Recommended Citation

Justin P. Williams, Ryan P. Hanavan, Barrett N. Rock, Subhash C. Minocha, and Ernst Linder. 2016. Influence of hemlock woolly adelgid infestation on the physiological and reflectance characteristics of eastern hemlock. Canadian Journal of Forest Research. 46(3): 410-426. https://doi.org/10.1139/cjfr-2015-0328

Canadian Journal of Forest Research
Revue canadienne de recherche forestière

Influence of Hemlock Woolly Adelgid Infestation on the Physiological and Reflectance Characteristics of Eastern Hemlock

Journal:	*Canadian Journal of Forest Research*
Manuscript ID	cjfr-2015-0328.R1
Manuscript Type:	Article
Date Submitted by the Author:	11-Dec-2015
Complete List of Authors:	Williams, Justin; USDA Forest Service, Southern Research Station Hanavan, Ryan; US Forest Service, Forest Health and Protection Rock, Barrett; University of New Hampshire, Earth Systems Research Center Minocha, Subhash; University of New Hampshire, Department of Biological Sciences Linder, Ernst; University of New Hampshire, Department of Mathmatics and Statistics
Keyword:	remote sensing, vegetation indices, fluorescence, chlorophyll, Adelges tsugae

Influence of Hemlock Woolly Adelgid Infestation on the Physiological and Reflectance Characteristics of Eastern Hemlock

Corresponding Author:

Justin P. Williams[1]: Department of Natural Resources and the Environment, James Hall, University of New Hampshire Durham, New Hampshire 03824 USA

Co-Authors:

Ryan P. Hanavan: U.S. Forest Service 271 Mast Rd. Durham, New Hampshire 03824 USA; rhanavan02@fs.fed.us

Barrett N. Rock: Earth Systems Research Center, Morse Hall, University of New Hampshire Durham, New Hampshire 03824 USA; rock.bg@comcast.net

Subhash C. Minocha: Department of Biological Sciences, Rudman Hall, University of New Hampshire Durham, New Hampshire 03824 USA; subhash.minocha@unh.edu

Ernst Linder: Department of Mathematics and Statistics, Kingsbury Hall, University of New Hampshire Durham, New Hampshire 03284 USA; elinder@unh.edu

[1] Current Affiliation: U.S. Forest Service Southern Research Station 775 Stone Blvd., Box 9861 Mississippi State, Mississippi 39762 USA; justinwilliams@fs.fed.us; Tel. (662) 325-8006

Abstract

The hemlock woolly adelgid (HWA) (*Adelges tsugae*) is an invasive insect in the eastern United States. Since its initial detection in Richmond, Virginia, in 1951, HWA has spread to half of the eastern hemlock natural range. Detection of early infestation symptoms via remote sensing requires the knowledge of the changes in reflectance resulting from physiological changes in the host as inflicted by the insect, and the selection of equipment with the appropriate sensor characteristics. Laboratory based reflectance measurements of infested and non-infested hemlock foliage collected from four sites in southern New Hampshire and Maine occurred biweekly over 6 months in 2012, and weekly over 5 weeks in 2013. Vegetation indices (REIP, NDVI, MSI and NIR3/1) were associated with concurrent chlorophyll and moisture content data. Infested first year foliage contained greater concentrations of chlorophyll and moisture resulting in reduced visible spectral reflectance, greater REIP and NDVI values, and lower MSI and NIR 3/1 values than non-infested foliage. Furthermore, fluorescence measurements indicated greater photosystem function during the early stages of infestation, suggesting a possible compensatory response by hemlock to infestation. Significant differences in reflectance between infested and non-infested foliage were observed in late June and July in the weeks immediately following HWA settlement on new growth. Implementing these observations during remote sensing mission planning may increase the likelihood of detecting early HWA infestation symptoms at landscape scales.

Keywords: *Adelges tsugae*, Hemlock Woolly Adelgid, remote sensing, vegetation indices, fluorescence, chlorophyll

1. Introduction

Eastern hemlock (*Tsuga canadensis* (L.) Carr.) is a foundation tree species in the northeastern United States (Ellison et al. 2005). Often found on steep slopes and in riparian areas, hemlocks filter water, retain soil, and provide shade to streams and habitat to wildlife (Bonneau et al. 1999). Currently, the vigor of the eastern hemlock population is declining due to multiple stressors like the elongate hemlock scale (Homoptera: *Fiorinia externa* Ferris), hemlock tip blight (*Sirococcus tsugae*), and more prominently the hemlock woolly adelgid (HWA) (Hemiptera: *Adelges tsugae* Annand).

Multiple studies have been published documenting the biology and ecology of HWA (McClure and Cheah 1999), its effects on needle chemistry (Radville et al. 2011), volatiles (Pezet et al. 2013), water and carbon relations (Domec et al. 2013), and radial growth (Davis et al. 2007). The effects of HWA infestation on hemlock reflectance features has received little attention, focusing only on airborne hyperspectral data collection and modeling (Hanavan et al. 2015, Pontius et al. 2005a, 2005b).

The purpose of this study was to examine the effects of HWA infestation on hemlock reflectance over time and how those changes related to leaf biophysical variables. The ultimate goal was to determine an optimal time period in the growing season for discrimination between infested and non-infested hemlock stands with either narrow or broadband remote sensing platforms. Our objectives were to:

1. Determine when hemlock reflectance was most affected by HWA infestation through both long (6 months) and short (5 weeks) term measurement intervals.

2. Determine whether HWA infestation impacted needle chlorophyll concentration and function through pigment extraction, reflectance and fluorescence measurements.

3. Determine whether HWA infestation impacted foliar moisture content through reflectance, fresh weight and dry weight measurements.

Health and growth of vegetation is dependent on the process of photosynthesis. Disruption of the photosynthetic apparatus leading to reduced plant vigor can be induced through a multitude of biotic and abiotic stressors. Insect infestations are a biotic stressor whereby feeding is accomplished through ingestion of foliage, phloem sap or xylem sap. Hemlock woolly adelgids feed from the xylem ray parenchyma cells which transfer water, nutrients and photosynthate solution, as well contain stored starch reserves within the parenchyma cell walls (Young et al. 1995). Feeding by HWA can cause premature needle drop, dieback of major limbs, and mortality within 4 to 15 years after infestation (McClure 1987). However, several studies of the effects of HWA on foliar chemistry have indicated that infested foliage had greater concentrations of nitrogen than non-infested foliage (Domec et al. 2013, Miller-Pierce et al. 2010, Pontius et al. 2006). Since foliar nitrogen is primarily bound to photosynthetic enzymes, those authors hypothesized that HWA infested trees may have greater photosynthetic capacity than non-infested trees. We set out to test those hypotheses through both direct (pigment extraction) and indirect (reflectance) measurements of chlorophyll concentration in infested and non-infested hemlock foliage. In addition, we evaluated photosystem integrity of infested and non-infested hemlock needles through fluorescence data to determine whether infestation affected overall chlorophyll function.

Reflectance properties of plants are controlled by pigments, cellular structure, and the amount of moisture filled intercellular air spaces contained within the spongy mesophyll (Gates et al. 1965). Changes in these properties due to HWA feeding would induce spectral shifts that could be compared to "healthy" spectra. In addition, many vegetation indices (VIs) that estimate biophysical parameters from spectral reflectance data have been developed; this project utilized four VIs to characterize possible differences in hemlock foliar health: Red Edge Inflection Point (REIP) (Horler et al. 1983), a measure of chlorophyll content; Normalized Difference Vegetation Index (NDVI) (Rouse et al. 1974), a measure of chlorophyll content and canopy biomass; Near Infrared (NIR) 3/1 Ratio (Bubier et al. 1997), a measure of foliar maturity; and the Moisture Stress Index (MSI) (Rock et al. 1986), a measure of leaf turgor.

Reflectance measuring sensors have the ability to detect canopy photosynthetic pigment and moisture statuses at varying spectral, spatial, and temporal resolutions. Identifying sensor traits that would be advantageous in detecting forests of declining health is paramount in remote sensing mission planning. We set out to determine how HWA infestation affected hemlock reflectance properties through changes in chlorophyll concentration and needle turgor, thereby inferring an appropriate spectral resolution for discriminating between HWA infested and non-infested forests. We also aimed to identify when the differences between infested and non-infested foliage were greatest by observing changes over time, thereby inferring the ideal timeframe for data collection and determining whether the duration of the spectral response would influence decisions concerning sensor temporal resolution. Given the potential for the rapid spread of HWA infestations due to its biannual and asexual lifecycle (McClure 1987), applying these observations to future remote sensing mission planning may increase the likelihood of detecting forests infested with HWA prior to major defoliation and or mortality.

2. Methods

2.1 *Defoliation Ratings*

Single 45 m radius plots were established at each of four locations (Fig. 1) (Table 1): Massabesic Experimental Forest in Alfred, Maine (N43.43927, W70.67931) which has been infested with HWA since 2012; Rachael Carson Wildlife Refuge on Cutts Island, Kittery, Maine (N43.09558, W70.67142) which has been infested with HWA since 2003; Russell-Abbott State Forest in Wilton, New Hampshire (N42.79048, W71.76155) which has been infested with HWA since 2011; and Northwood Meadows State Park in Northwood, New Hampshire (N43.20466, W71.19827) where HWA presence had not yet been detected as of 2015. Plots were established in June 2012; all trees 10 cm diameter at breast height (DBH) and over were measured, and each hemlock was given a unique identification number and rated for defoliation. Defoliation ratings were estimated based on the percent defoliation of the live crown: 1 = < 25% defoliation; 2 = 26 - 50% defoliation; 3 = 51 -75% defoliation; 4 = 76 - 99% defoliation; 5 = 100% defoliation (dead) (Orwig & Foster 1998). Defoliation ratings were determined through consensus by a two-person crew. The same crew was used to rate every tree in this study.

2.2 *2012 Reflectance and Spectral Indices*

In 2012 hemlock foliage from plots were sampled bi-weekly from the end of June (post HWA emergence) through the second week of December. Two tagged hemlocks were chosen randomly at each plot; due to the lottery style selection of numbers some hemlocks were sampled more than once over the seven month period. Light-exposed terminal hemlock branches were sampled with pole pruners from the lower, middle, and upper live crown in each cardinal direction. Samples were stored and transported to the lab in coolers with blue ice. Infestation

123 status was determined by thoroughly checking each sample for signs of HWA. Samples were
124 then separated into first year and second year branch segments for spectral analysis. Reflectance
125 measurements were taken within 24 to 48 hours of foliage being cut from the tree. Foliage was
126 frozen for pigment extractions following spectral analysis.

127 First and second year branch segments were separately arranged, in an optically dense
128 layer, in petri dishes spray painted in flat black color. Spectral reflectance was measured using a
129 Visible InfRared Intelligent Spectrometer (VIRIS GER 2600; Geophysical Environmental
130 Research Corporation, Millbrook, NY, USA); a spectralon-coated hemispherical/baffle light
131 source of 30W tungsten and halogen light bulbs was set at a 45 degree angle 50 cm from the
132 sample (Rock et al. 1994). Distance from the optical lens of the spectrometer to the sample was
133 50 cm yielding a field of view of approximately 7 cm^2. The spectrometer measured reflectance
134 from 400 to 1000 nanometers in approximately 2 nm steps, and from 1000 to 2500 nm in
135 approximately 12 nm steps. Visible light reflectance was measured from 400 to 680 nm, NIR
136 reflectance from 750 to 1400 nm, and middle infrared reflectance (MidIR) from 1400 to 2500 nm
137 (Gates et al. 1965, Gausman 1977). The red edge spectral region was defined as 680 to 750 nm
138 (Horler et al. 1983). Each sample was scanned three times with a 90 degree rotation in between
139 measurements. The three scans were averaged; estimated Landsat Thematic Mapper (TM) band
140 values and VIs were calculated and tabulated using ProVIRIS Software (Shannon Spencer,
141 Copyright 2000).

142 Vegetation indices of immediate interest were the REIP, NDVI, MSI, and NIR 3/1 ratio.
143 The REIP, an estimator of chlorophyll content, was determined as the wavelength at which the
144 first derivative curve between 680 and 750 nm reached its maximum peak (Horler et al. 1983).
145 The NDVI, an estimator of canopy biomass and leaf chlorophyll content, was calculated using

estimated Landsat red (B3) and NIR (B4) bands (B4 – B3/B4 + B3) (Rouse et al. 1974). The MSI, an estimator of foliar water content, was calculated using estimated Landsat NIR and MidIR (B5) bands (B5/B4) (Rock et al. 1986). The NIR 3/1 ratio, an estimator of foliar maturity, was calculated as the slope of the NIR plateau (Bubier et al. 1997). Indices and spectra data from all sites were pooled by infestation status (infested or non-infested) and then averaged for each month; any non-infested samples from trees that were later determined to be infested were excluded. Site to site variation in the 2012 data was not specifically addressed due to the majority (79.7%) of infested samples coming from the Rachael Carson National Wildlife Refuge. Statistical differences between infested and non-infested foliage were tested for both the spectra and the VIs using Wilcoxon's Tests in JMP (JMP Pro Version 10.0. SAS Institute Inc., Cary, NC, 1989-2007). Reflectance difference (infested minus non-infested) and sensitivity (reflectance difference divided by non-infested) curves were used to highlight portions of the hemlock reflectance spectrum most affected by HWA infestation (Carter 1993).

2.3 *2013 Reflectance and Spectral Health Indices*

In 2013, only trees at the Massabesic Experimental Forest were sampled. Sampling in 2013 was reduced to one site in order to limit differences between sites as a possible confounding factor from 2012 data. In addition, sampling began two weeks prior to HWA emergence allowing us to observe infestation impacts before and after HWA settlement on first year growth. Five non-infested and five HWA infested hemlock of similar DBH (51.5 ± 9.8 cm) were selected. Sunlit terminal branches of each hemlock were sampled over a five week period from 4 June to 1 July using pole pruners or a 12-guage shotgun with steel shot. Only foliage not impacted by the shot was used. Following transport to the lab foliar fluorescence measurements were taken.

After the fluorescence measurements were conducted, reflectance measurements and statistical analysis of first year foliage were performed using the same protocols described for the 2012 sampling period. Following reflectance measurements the very top layer of foliage was used for pigment extraction; only the top layer was used in an effort to limit variation in correlating VIs with chlorophyll concentrations. Linear regression was performed in JMP 10.0 with total chlorophyll as the independent variable and the REIP and NDVI values as the dependent variables.

2.4 *Chlorophyll Extraction and Fluorescence*

Following the 2012 sampling period frozen foliage from June, July and August were used in pigment extractions. For each tree needle year, approximately 0.5 g of needle material was scissors chopped into a petri dish and homogenized. Approximately 0.1 g of the needle mixture was placed into a centrifuge tube with 10 mL of 95% ethyl alcohol (ETOH) and incubated in a 60° C water bath for 16 hours (Minocha et al. 2009). Extractions were cooled to room temperature in the dark and transported to a separate lab in a cooler. Samples were centrifuged for five minutes at 5000 revolutions per minute (RPM). Approximately 2 mL of extract were pipetted into 3 mL quartz cuvettes (n = 5 for each tube); absorbance was measured using a Genesys 6 (Fisher Scientific) spectrophotometer at 470, 649, and 664 nm. Chlorophylls (*a*, *b* and total) and total carotenoid concentrations were calculated using equations from Lichtenthaler (1987). Pigment extraction protocols for the 2013 samples were slightly different. Approximately 0.05 g of fresh needle material per sample was scissors chopped into each of two centrifuge tubes and frozen immediately following reflectance measurements. Extractions took place in July 2013. Tubes were pulled from the freezer and 5 mL of ETOH was added; approximately 2 mL of extract were pipetted into 3 mL quartz cuvettes (n = 2 for each tube).

Absorbance measurements and pigment concentration calculations followed the same protocols as the 2012 samples.

Prior to fluorescence measurement five clips (per sample) were attached to infestation intensity representative needles for a 20 minute dark adaptation period; fluorescence measurements were taken within 4 hours of branches being removed from the tree. The Handy PEA Fluorimeter (Hansatech Instruments Limited; Norfolk, UK) measured fluorescence induced in a 12.6 mm^2 area by exposing it to a saturating red actinic light intensity of 1500 $\mu Mol\ m^{-2}\ s^{-1}$ for a duration of 1 second. Fluorimeters such as the Handy PEA measure the polyphasic rise in chlorophyll fluorescence of photosystem II (PSII), providing quantitative and qualitative interpretations of active processes within the photosynthetic apparatus. Fluorescence intensity measurements were used in the multiparametric JIP Test (Strasser et al. 2000, 2004). Statistical differences in parameters were analyzed using Wilcoxon's Tests in JMP 10.0; here we report only on parameters Fv/Fm which is the maximum quantum efficiency of PSII; the Absorbance Performance Index (PIabs) which is a measure of plant vitality that examines the quantity of reaction centers, the maximum energy flux that reaches the reaction centers of PSII, and electron transport; and the Total Performance Index (PItot) which extends the PIabs parameter to include reductions at the electron acceptor site of PSI (Perboni et al. 2012).

2.5 *Fresh and Dry Weight*

After fluorescence and reflectance measurements were taken, and the top foliage reserved for pigment extraction, fresh weight of the sample was measured. Twigs with attached foliage were then dried at 50 degrees Celsius for seven days in a brown paper bag. Dry weight for the sample was then recorded. Differences in foliar moisture content (fresh weight minus dry

weight) were analyzed using Wilcoxon's Tests in JMP 10.0. Correlation of foliar moisture content to the MSI was calculated in JMP 10.0.

3. Results

3.1 *Defoliation Ratings*

Hemlocks at the Massabesic Experimental Forest had an average defoliation rating of 1.58 ± 0.68 (N = 93). Of first year foliage sampled from 25 hemlock crowns, 24.6% were infested with HWA (Table 2). Hemlocks at the Rachael Carson Wildlife Reserve had an average defoliation rating of 1.14 ± 0.43 (N = 63). Of the first year growth sampled from 23 hemlock crowns, 96.9% were infested with HWA (Table 2). At the Russell-Abbott State Forest the average hemlock defoliation rating was 1.33 ± 0.94 (N = 82). Of the first year growth sampled from 24 trees, 4.5% were infested with HWA (Table 2). At Northwood Meadows State Park HWA all samples from 23 trees were not infested with HWA (Table 2). The average hemlock defoliation rating was 1.21 ± 0.73 (N = 210).

3.2 *2012 Reflectance and Spectral Health Indices*

Reflectance values of first year infested foliage were consistently lower than non-infested foliage in the visible (400 – 680 nm) and red edge (680-750 nm) portions of the spectrum during the seven month sampling period. Differences in visible light reflectance were greatest near the green peak (~ 550 nm). Infested foliage green peak values ranged from 0.1 to 2.5% lower than non-infested foliage; the greatest differences occurred in June (2.6%) and July (2.0%) post HWA settlement (Fig. 2A, 2C). Infested foliage red edge (680-750 nm) reflectance values ranged from 0.8 to 4.6% lower than non-infested foliage, indicating a shift of the red edge to longer wavelengths. The greatest differences in the red edge region also occurred in June (4.5%) and

July (3.5%) (Fig. 2A, 2C). For the remaining months green peak differences were less than 1.3% and red edge differences were less than 2.4%.

Statistical differences between current year infested and non-infested foliage in the visible and red edge regions were most notable in June and July (Fig. 3A, 3C). In June, 28 bands from 400 to 494 nm, 32 bands from 500 to 547 nm, and 21 bands from 648 to 679 nm comprised the 81 total bands across the visible portion of the spectrum that were significantly different ($P < 0.05$) (Table 3). The most significant ($P < 0.01$) bands in the visible region were at 493 and 502 nm. In the red edge region 37 bands were found to be significantly different ($P < 0.05$) (Table 3). The most significant ($P < 0.01$) bands were from 721 to 729 nm; six consecutive bands that were each approximately 2 nm wide. In July, 50 bands from 500 to 596 nm and 7 bands from 604 – 635 nm comprised the 57 total bands across the visible portion of the spectrum that were significantly different ($P < 0.05$) (Table 3). The most significant ($P < 0.01$) bands in the visible region were at 520, 525, and 543 nm. Only one band in the red edge at 705 was found to be significantly different ($P = 0.04$).

Differences in NIR reflectance (750 – 1400 nm) ranged from 3.0% lower than non-infested foliage in June (Fig. 2A) to 2.0% higher than non-infested foliage in September, October and November (Fig. 2G, 2I, 2K). No statistical differences between infested and non-infested foliage in the NIR region were observed (Table 3) (Fig. 3). Differences in MidIR reflectance (1400 - 2400 nm) values ranged from 1.8% lower than non-infested foliage in October (Fig. 2G) to 0.1% higher than non-infested foliage in December (Fig. 2K). Statistical differences ($P < 0.05$) between infested and non-infested foliage in the MidIR region occurred in July (2049, 2293, 2305, and 2364 nm), August (2434 nm), October (2305 nm), November (2281 nm), and December (2329 and 2446 nm) (Table 3) (Fig. 3C, 3E, 3I, 3K, 3M).

Sensitivity to infestation (reflectance difference divided by non-infested reflectance; Fig. 2) of first year foliage was greatest in both the visible and red edge spectral regions for all months observed except for October (Fig. 2J) when the MidIR reflectance region had the greatest sensitivity. The greatest sensitivity to infestation for first year growth was observed in late June and July. In the visible light reflectance region, sensitivity in June and July was greatest from approximately 500 to 650 nm (Fig. 2B, 2D). In the red edge region, sensitivity was greatest at approximately 700 nm (Fig. 2B, 2D).

Second year foliage reflectance difference values were inconsistent compared to current year reflectance differences. Differences in visible light reflectance were greatest near the green peak; values ranged from 0.4% lower than non-infested foliage in June (Fig. 4A) to 0.3% higher in October (Fig. 4I). Red edge spectral region values ranged from 2.2% lower than non-infested foliage in September to 2.7% higher in July (Fig. 4A, 4C). Differences in NIR reflectance ranged from 2.6% lower than non-infested foliage in September to 3.1% higher in July (Fig. 4C, 4G). Middle infrared reflectance values of infested foliage were consistently lower than non-infested foliage from June through November (Fig. 4A, 4C, 4E, 4G, 4I, 4K) and difference values ranged from 2.3% lower in September (Fig. 4G) to 1.7% higher in December (Fig. 4M).

Statistical differences between second year infested and non-infested foliage were greatest in the visible spectral region in July (Fig. 3D). In July, 13 bands from 400 to 494 nm and 5 consecutive bands from 503 to 515 nm comprised the 18 total bands across the visible portion of the spectrum that were statistically significant ($P < 0.05$) (Table 3). The only band in the red edge region that was significantly different was at 687 in August ($P = 0.03$) (Fig. 3F). In the NIR region three consecutive significantly different bands were observed in November (1369, 1383, and 1397) (Fig. 3L); two of those bands were also significantly different in

December (1383 and 1397) ($P < 0.05$) (Fig 3N). More notable was the number of significantly different bands in the MidIR spectral region in November (26 bands from 1411 to 2305 nm)) (Fig. 3L) and December (37 bands from 1411 to 2411nm) (Fig 3N) ($P < 0.05$) (Table 3).

Sensitivity to infestation of second year foliage in the visible and red edge spectral regions varied month to month and was inconsistent compared to first year foliage. Sensitivity near the green peak was greatest in June, August, September and November (Fig. 4B, 4F, 4H, 4L). Sensitivity in the red edge region was greatest in June and December at approximately 700 nm (Fig. 4B, 4N). Sensitivity in the MidIR was greater than sensitivity in the visible, red edge and NIR spectral regions for all months sampled except for August (Fig. 4B, 4D, 4F, 4H, 4J, 4L, 4N).

Mean REIPs of first year infested foliage were consistently higher than non-infested foliage over the sampling period (Fig. 5A). Mean REIPs of first year foliage were statistically greater only in December ($P = 0.04$) (Table 4). Second year growth mean REIPs for infested foliage were not statistically different from non-infested foliage (Fig. 5B). Like the REIP, mean NDVI values for first year infested foliage were generally higher than non-infested foliage (Fig. 5C), but were never statistically different. No significant differences in mean NDVI values for second year infested foliage were observed (Table 4).

Both first year and second year infested foliage generally had lower mean MSI values than non-infested foliage (Fig. 5E, 5F). First year foliage was found to have statistically lower mean MSI values in October ($P = 0.01$) and November ($P = 0.02$) (Table 4). Second year infested foliage had statistically lower mean MSI values in July ($P = 0.03$), October ($P = 0.03$), and November ($P = 0.03$) (Table 4).

Infested first year and second year foliage exhibited both higher and lower mean NIR 3/1 ratio values compared to non-infested foliage (Fig. 5G, 5H). First year foliage had statistically lower NIR 3/1 values in October ($P = 0.01$) and November ($P = 0.02$) (Table 2). Mean June NIR 3/1 ratio values for second year foliage were not statistically different (Fig. 5H). Mean NIR 3/1 ratio values for second year foliage were statistically lower than non-infested foliage the months of August ($P = 0.03$), October ($P = 0.01$), and November ($P = 0.02$) (Table 2).

3.3 *2013 Reflectance and Spectral Health Indices*

Hemlock woolly adelgids began to emerge at Massabesic Experimental Forest the week of 10 June, and by 17 June HWA crawlers were present on first year growth of infested trees. Improper sampling the week of 24 June resulted in only three samples of infested first year growth. Infested foliage had consistently lower visible and red edge reflectance values than non-infested foliage; the greatest differences occurred the week of 1 July (Fig. 6I) two weeks after HWA settlement. Differences in green peak reflectance values ranged from 2.9% lower than non-infested foliage on 1 July (Fig. 6I) to 1.0% higher on 17 June (Fig. 6E). Differences in red edge region reflectance values ranged from 3.8% lower than non-infested foliage on 1 July (Fig. 6I) to 0.2% higher on 24 June (Fig. 6G). Differences in NIR reflectance values ranged from 3.0% lower than non-infested foliage on 10 June (Fig. 6C) to 12.1% higher on 24 June (Fig. 6G). Differences in MidIR reflectance values ranged from 2.5% lower than non-infested foliage on 10 June (Fig. 6C) to 2.5% higher on 4 June (Fig. 6A).

Statistical differences between infested and non-infested foliage were greatest the week of 1 July (Table 5). In the visible portion of the spectrum 37 bands from 504 to 598 nm and 7 bands from 604 to 637 nm comprised the 44 total bands that were significantly different ($P <$

0.05) (Table 5) (Fig. 7E). In the red edge region, 12 significantly different bands were observed from 691 – 714 nm ($P < 0.05$). Four bands in the MidIR region (2305, 2364, 2388, and 2481) were also significantly different ($P < 0.05$) (Table 5) (Fig. 7E). Significant differences were also observed the week of 17 June in the NIR spectral region, in all twenty-eight bands from 961 to 1311 nm were significantly greater than non-infested foliage ($P < 0.05$) (Table 5) (Fig. 7C).

Sensitivity to infestation was greatest in both the visible and red edge spectral regions the week of 1 July, approximately two weeks after HWA settlement on new hemlock growth. Sensitivity in the visible portion of the spectrum was greatest from 515 to 637 nm (Fig. 6J), and in the red edge region sensitivity peaked at approximately 700 nm. In the NIR and MidIR spectral regions sensitivity was greatest the week of 24 June.

Infested foliage generally had higher mean REIP and NDVI values over the five week sampling period (Fig. 8A, 8B). Statistically greater mean REIP values were observed on 1 July ($P = 0.01$) (Table 6). Statistically greater mean NDVI values were observed on 4 June ($P = 0.02$) and 1 July ($P = 0.02$) (Table 6). Moisture Stress Index (MSI) and NIR 3/1 values were not statistically different between infested and non-infested foliage (Table 6) (Fig. 8C, 8D).

3.4 *Chlorophyll Extraction and Fluorescence*

First year growth of infested trees in 2012 generally had higher mean concentrations of all measured pigments than non-infested trees, but significantly greater concentrations were not observed (Table 7). Photosynthetic pigment values in second year growth also did not differ between infested and non-infested foliage (Table 7).

First year growth of infested trees in 2013 from the Massabesic Experimental Forest generally had higher mean concentrations of all measured pigments than non-infested trees,

348 although not always statistically greater (Fig. 9). Statistically greater concentrations of
349 chlorophyll *a* were observed on 4 June ($P = 0.04$) and 1 July ($P = 0.02$), and chlorophyll *b* on 17
350 June ($P = 0.05$) (Table 8). Statistically greater concentrations of total carotenoids was observed
351 on 4 June ($P = 0.01$) and 24 June ($P = 0.04$) (Table 8). Total chlorophyll was not statistically
352 different between infested and non-infested foliage. Total chlorophyll concentration had a
353 positive linear relationship to the REIP ($r^2 = 0.81$, df = 1, 48, $F = 204.95$, $P < .0001$); the natural
354 log of total chlorophyll was positively related to the NDVI ($r^2 = 0.89$, df = 1, 48, $F = 469.25$, $P <$
355 .0001).

356 Infested hemlock foliage showed no statistical differences in Fv/Fm compared with non-
357 infested foliage over the five week sampling period (Fig. 9C) (Table 9). Statistically greater
358 PIabs for infested foliage was observed on 4 June ($P = 0.05$), 24 June ($P = 0.01$) and 1 July ($P =$
359 0.0002) (Fig. 10B) (Table 9). Infested foliage also had statistically greater PItot the weeks of 4
360 June ($P = 0.02$), 10 June ($P = 0.006$), 24 June ($P = 0.004$) and 1 July ($P < 0.0001$) (Fig. 10A)
361 (Table 9).

362 **3.5 *Fresh and Dry Weight***

363 Moisture content (fresh weight minus dry weight) of infested foliage did not differ
364 statistically from non-infested foliage (Fig. 11A). The MSI was found to be negatively
365 correlated with needle moisture content values ($r = -0.43$, $P = 0.002$) (Fig. 11B).

366 **4. Discussion**

367 Although past studies using Landsat TM data, VIs, and transformations to map high-
368 severity HWA-induced defoliation have been successful (Bonneau et al. 1999, Royle & Lathrop
369 2002), currently, those approaches may not be suitable for these study areas. Among the four

sites mean defoliation was less than 26% regardless of HWA presence. The Rachael Carson Wildlife Refuge was the oldest reported infestation and the most heavily infested; however, it was also the least defoliated based on field ratings (1.14 ± 0.43). The Massabesic Experimental Forest plot, although being newly infested, had the highest defoliation average of 1.58 (± 0.68). To conclude that no relationship between infestation intensity and defoliation existed based on four sites would be presumptuous; however, hemlock defoliation and mortality as seen in the Mid-Atlantic and southern New England states had not yet occurred at these site locations.

The apparent lack of defoliation and mortality that is commonly associated with HWA infestation may be partially explained by site geographic location. Orwig et al. (2012) found that the severity of damage caused by HWA was negatively correlated with latitude; however, damage could be exacerbated by drought and site exposure conditions. The latitude damage gradient is in part due to cold winter temperatures which causes HWA mortality, upwards of 90% locally (Trotter and Shields 2009), thereby retarding HWA population growth in newly infested stands and extending the timeframe to significant defoliation and mortality. These semi-annual reductions in HWA populations in concert with site characteristics favorable to hemlock also induce year to year cycles of hemlock recovery and decline in chronically infested stands (Mayer et al. 2002). Regardless of annual fluctuations in winter temperatures positively or negatively influencing HWA populations and cycles of hemlock decline and recovery, significant defoliation in this region had been limited as of 2014 and therefore changes in biomass values alone may not be adequate in detecting early infestation symptoms.

Spectral difference and sensitivity curves indicated that late June and early July (post HWA emergence) may be the optimal time of year to discriminate between HWA infested and non-infested forests with reflectance measuring sensors. Reflectance difference and sensitivity

curves of first year foliage from both 2012 and 2013 indicated that the visible and red edge spectral region reflectance values of infested foliage were consistently lower than non-infested foliage during that time period, and that those spectral regions would be the most sensitive in detecting infestation. Statistically lower reflectance values were observed across multiple bands in the visible and red edge spectral regions. In June and July of 2012 a combined 118 different bands from 400 – 680 nm (~2 nm bandwidths), and 37 different bands from 680 – 736 nm along the red edge (~2 nm bandwidths), were found to be significantly different between infested and non-infested foliage. A similar pattern was observed the week of 1 July in 2013 when 44 bands in the visible and 12 bands in the red edge spectral regions were significantly different. Additionally, second year infested foliage in July of 2012 had significantly lower reflectance values at 18 different bands from 400 – 515 nm. These observations agree with numerous other studies that have shown that the visible and red edge regions of the reflectance spectrum are the most affected by and sensitive to plant stress due to changes in foliar pigment concentrations (Carter 1993, Carter & Knapp 2001, Gitelson et al. 1996, Rock et al.1988). However, considering that forest canopy remote sensing data typically consists of mixed pixels containing multiple trees (and tree species), layers of foliage, foliage growth years and woody material, the significance of the spectral differences observed in the data may be subdued at moderate and low spatial resolutions.

The patterns observed in the current year foliage reflectance data correspond well with the sisten crawler and aestivation (summer dormancy) phases of the HWA lifecycle. Hemlock woolly adelgids have two generations per year, the progrediens which hatch in March and the sistens which hatch in June (for a detailed study of the HWA lifecycle see McClure and Cheah 1999). Our data cover the majority of the sisten generation. The greatest observed differences in

reflectance occurred in late June and July in the weeks following the emergence of sisten HWA crawlers and their settlement at the base of new growth. During that time significantly lower visible spectral reflectance, shifts of the red edge to longer wavelengths, and lower MidIR reflectance were observed. In August, when the HWA nymph is reported to begin aestivation and feeding pauses until October, differences in the visible and red edge regions reduced substantially before rebounding in November and December when adelgid feeding and growth resumed. It is not clear whether the physiological and spectral responses were driven by HWA influencing source-sink dynamics within the tree (Gómez et al. 2012) or were induced by enzymes released by the HWA (Oten et al. 2014).

The aestivation period was also characterized by greater NIR reflectance from infested foliage August through November. Leaf reflection in the NIR spectral region is due to light refraction at cell wall and intercellular air space interfaces (Gates et al. 1965); generally, higher NIR reflectance is associated with healthier vegetation and older conifer needle years (Rock et al. 1994). The reasons why NIR reflectance of current year infested foliage jumped from being approximately 3% lower than non-infested foliage in July, to approximately 2% higher than non-infested foliage in November, and finally no different from non-infested foliage in December, remain unclear without leaf anatomical evaluation. However, it is possible that the lapse in HWA feeding resulted in a period of rapid growth and expansion of intercellular airspaces, thereby increasing NIR reflectance.

Patterns in the second year foliage reflectance data did not correspond as well with the HWA lifecycle. The reason for this was unknown, although chronic infestation and its effects on foliar metabolism may explain the month to month variability in reflectance values. Significant differences in reflectance in the visible, red edge and MidIR portions of the spectrum were

observed before and after aestivation. Before aestivation, significant differences in the visible and red edge spectral regions occurred in July and August; perhaps a delayed response to sisten HWA feeding on the newer foliage. After aestivation, significant differences were observed in the MidIR spectral region in November and December, signaling changes in foliar moisture content.

The data indicated that although the REIP may be highly correlated to needle chlorophyll content, use of the REIP alone in detecting HWA infestations may not be suitable because differences in chlorophyll content between newly infested and non-infested trees may not be significant or consistent, because of differences in recovery and decline cycles at chronically infested sites, and because other wavelengths along the red edge may be more sensitive. For example, in June 37 consecutive bands along the red edge from 680 to 736 nm were significantly different between infested and non-infested foliage including the wavelength at which their respective REIPs occurred (718 nm); however, there were no significant differences in chlorophyll content or REIP. This is because a significant difference in percent reflectance at the wavelength at which the REIP occurs does not translate into significantly different REIPs; the two measurements are mutually exclusive. In addition there were six bands from 721 – 729 nm where the greatest statistical differences in the red edge occurred, that likely would have been more important than the REIP in detecting infested hemlock. Therefore, in choosing the appropriate sensor for detecting HWA infestations, a sensor with wider (> 2 nm) bands along the red edge may be just as useful as a sensor with very narrow (≤ 2 nm) bands from which the REIP can be determined.

Needles of infested hemlock exhibited reduced spectral maturity over time compared with non-infested hemlock. The mean NIR 3/1 ratio values of infested first year needles were

initially greater than non-infested needles in June 2012. However, first year needles had statistically lower mean NIR 3/1 ratio values in October and November, and second year needles had statistically lower mean NIR 3/1 ratio values in August, October and November. The 2013 NIR 3/1 ratio values exhibited a similar short term pattern. Mean NIR 3/1 ratio values were greater in the first sampling week but lower in the remaining four sampling weeks, although never statistically significant. These patterns indicated that infested hemlock needles may have had a more difficult time reaching the same cellular and structural maturity of non-infested hemlock needles; however, anatomical data would be needed to reach definitive conclusions. In addition, a possible confounding link between the NIR 3/1 ratio and leaf turgidity cannot be ignored as the patterns in the MSI and NIR 3/1 indices were similar (Hunt and Rock 1989).

Hemlock foliage impacted by HWA generally had higher moisture content (i.e. lower MSI values) than non-infested foliage over the seven month period. Significantly lower MSI values were observed in October and November for both current year and second year foliage which corresponds with HWA breaking aestivation. However, only a moderate correlation (r = -0.43) of the MSI to needle moisture content was observed. This indicated that although the MSI may have had some usefulness in discriminating between infested and non-infested hemlock foliage, it was not a highly accurate gauge of needle turgidity. Regarding the remote sensing of hemlock canopies, the supposed increase in turgidity and differences in MSI values that were observed between infested foliage and non-infested foliage may not extend to sub-mesic sites where water availability is low or to chronically infested sites during decline cycles.

Hemlock woolly adelgid infestation undoubtedly negatively affects hemlock health in the long term; however, our data suggest a possible compensatory increase in photosynthetic machinery and function in new growth during the early stages of infestation. This increase was

485 observed through both direct and indirect chlorophyll measurements. Increased chlorophyll
486 content was directly measured through pigment extraction and determination of concentration
487 through well-established methods (see Lichtenthaler 1987, Minocha et al. 2009). Indirect
488 measurements of increased chlorophyll concentration and function were accomplished through
489 VIs (REIP and NDVI) and fluorescence measurements. Both pigment extraction and reflectance
490 measurements of infested foliage had consistently higher mean chlorophyll concentrations, some
491 of which means were significantly greater than non-infested foliage. In addition, fluorescence
492 measurements indicated that the chlorophyll in infested foliage was functioning properly
493 (Fv/Fm), and that infested foliage was absorbing more photon energy (PIabs) than non-infested
494 foliage due to increased chlorophyll concentrations, resulting in greater overall photosynthetic
495 capability (PItot) in terms of machinery.

496 The increase in photosystem capability in HWA infested hemlock, as indicated through
497 the pigment extraction, reflectance and fluorescence data, may be the result of several factors.
498 First, Gómez et al. (2012) documented that after the first year of HWA infestation total amino
499 acid concentration in new un-infested foliage was 330% greater than in the control treatment.
500 Whether the increase in free amino acids was either a manipulation of the host species by HWA
501 or a systemic compensatory response whereby N was reallocated from stressed to non-stressed
502 foliage was unknown; regardless, our data suggests that an increase in N may have resulted in
503 greater concentrations of chlorophyll. Second, water stress in plants has been shown to increase
504 foliar N availability and decrease photosynthetic capacity. Gonda-King et al. (2014) reported
505 that HWA infested hemlock seedlings (< 3ys age) had greater negative water potential (i.e. were
506 water stressed) resulting in greater total N content, decreased stomatal conductance, and
507 decreased net photosynthesis in a controlled experiment. Our MSI data from mature hemlocks

indicated that infested foliage was less water stressed than non-infested foliage and that water was likely not a limiting factor for photosynthesis. Although it was possible that the combination of greater availability of nitrogen and water produced a temporary increase in photosystem machinery and function in the new flush of foliage, stomatal conductance was not measured and therefore we cannot state with certainty that the increased photosynthetic machinery resulted in greater photosynthetic rates (Rubino et al. 2015).

5. Conclusion

Sensor selection and timing of remote sensing data collection are important aspects of project planning. To discriminate between incipient HWA infested and non-infested hemlock stands aerial spectrometers measuring reflectance in the visible and red edge spectral regions over narrow bandwidths (~2 nm) would be best; however, aerial and satellite multispectral sensors with wider bandwidths may be sufficient. Perhaps more importantly, our data suggest that projects involving on-demand aerial data collection should time collection efforts in the weeks immediately following sisten adelgid emergence in June; projects that involve gathering of previously acquired satellite data should focus on late June or July. Acquiring data outside of this window may reduce the likelihood of successful discrimination between infested and non-infested hemlock stands.

These recommendations are based on the reflectance data which showed that in late June and early July infested foliage were most significantly different from non-infested foliage in the visible and red edge spectral regions. These peaks in spectral differences constitute peaks in sensitivity, the ability of the sensor to distinguish between infested and non-infested hemlock forests. In all 118 different wavelengths in the visible spectral region and 37 different

wavelengths along the red edge were observed to be significantly different. The high number of significantly different wavelengths indicated that sensors measuring in either narrow (hyperspectral) or wide band widths (i.e. aerial and satellite multispectral data) in the visible and red edge wavelengths may have the ability to detect early infestations. Our data also suggest that wavelengths or indices that correlate with leaf turgidity and chlorophyll content may be useful in discriminating between HWA infested and non-infested forests. Infested foliage was found to have contained greater concentrations of both chlorophyll and moisture, although the differences were not always statistically significant. Furthermore, our data support the view of a compensatory response to initial infestation in current year foliage, although the mechanism triggering this response was unclear.

Acknowledgements: This research was a portion of a thesis submitted to the Graduate School of the University of New Hampshire as part of the degree requirements of a Master's of Science in Natural Resources. Funding for this project was provided through the United States Department of Agriculture Forest Service (Forest Health and Protection), New Hampshire Space Grant Consortium, University of New Hampshire Farrington Fund Fellowship and College Woods Scholarship, and the Bearcamp Valley Garden Club Scholarship. Marc DiGirolomo, Angela Hammond, Michael Simmons, Michael Bohne, Robert Cooke, Edward Jordan, Kevin Dodds, and Garret Dubois of the USFS provided field support. We would also like to thank David Orwig for his comments on an earlier version of this manuscript, and the anonymous reviewers for their comments and suggestions.

References:

Bonneau, L. R., Shields, K. S., and Civco, D. L. 1999. Using satellite images to classify and analyze the health of hemlock forests infested by the hemlock woolly adelgid. Biol. Invasions **1**: 255–267.

Bubier, J. L., Rock, B. N., and Crill, P. M. 1997. Spectral Reflectance Measurements of Boreal Wetland and Forest Mosses. J. Geophys. Res. **102**(D24): 29,483–29,494.

Carter, G. A. 1993. Responses of Leaf Spectral Reflectance to Plant Stress. Bot. Soc. Am. **80**(3): 239–243.

Carter, G. A., and Knapp, A. K. 2001. Leaf Optical Properties in Higher Plants : Linking Spectral Characteristics to Stress and Chlorophyll Concentration. Bot. Soc. Am. **88**(4): 677–684.

Davis, D. D., Fromm, M. S., and Davis, M. D. 2007. Impact of the Hemlock Woolly Adelgid on Radial Growth of Eastern Hemlock in Pennsylvania. pp. 157–162 Proceedings of the 15th Central Hardwood Forest Conference. USDA Forest Service, Gen. Tech. Rep. SRS-101.

Domec, J.-C., Rivera, L. N., King, J. S., Peszlen, I., Hain, F., Smith, B., and Frampton, J. 2013. Hemlock woolly adelgid (Adelges tsugae) infestation affects water and carbon relations of eastern hemlock (Tsuga canadensis) and Carolina hemlock (Tsuga caroliniana). New Phytol. **199**(2): 452–63. doi:10.1111/nph.12263.

Ellison, A. M., Bank, M. S., Clinton, B. D., Colburn, E. A., Elliott, K., Ford, C. R., Foster, D. R., Kloeppel, B. D., Knoepp, J. D., Lovett, G. M., Mohan, J., Orwig, D. A., Rodenhouse, N. L., Sobczak, W. V., Stinson, K. A., Stone, J. K., Swan, C. M., Thompson, J., Von Holle, B., and Webster, J. R. 2005. Loss of Foundation Species: Consequences for the Structure and Dynamics of Forested Ecosystems. Front. Ecol. Environ. **3**(9): 479–486.

Gates, D. M., Keegan, H. J., Schleter, J. C., and Weidner, V. R. 1965. Spectral Properties of Plants. Appl. Opt. **4**(1): 11–20.

Gausman, H. W. 1977. Reflectance of leaf components. Remote Sens. Environ. **6**(1): 1–9. doi:10.1016/0034-4257(77)90015-3.

Gitelson, A. A., Merzlyak, M. N., and Lichtenthaler, H. K. 1996. Detection of Red Edge Position and Chlorophyll Content by Reflectance Measurements Near 700 nm. J. Plant Physiol. **148**: 501–508. doi:10.1016/S0176-1617(96)80285-9.

Gómez, S., Orians, C. M., and Preisser, E. L. 2012. Exotic herbivores on a shared native host: tissue quality after individual, simultaneous, and sequential attack. Oecologia **169**(4): 1015–24. doi:10.1007/s00442-012-2267-2.

Gonda-King, L., Gómez, S., Martin, J. L., Orians, C. M., and Preisser, E. L. 2014. Tree responses to an invasive sap-feeding insect. Plant Ecol. **215**(3): 297–304. doi:10.1007/s11258-014-0298-y.

Hanavan, R. P., Pontius, J., and Hallett, R. 2015. A 10-Year Assessment of Hemlock Decline in the Catskill Mountain Region of New York State Using Hyperspectral Remote Sensing Techniques. J. Econ. Entomol.: 1–11. doi:10.1093/jee/tou015.

Horler, D. N. H., Dockray, M., Barringerj, A. R., and Barber, J. 1983. Red Edge Measurements for Remotely Sensing Plant Chlorophyll Content. Plant Physiol. **3**: 273–277.

Hunt, E. R., and Rock, B. N. 1989. Detection of Changes in Leaf Water Content Using Near- and Middle-Infrared Reflectances. Remote Sens. Environ. **30**: 43–54.

Lichtenthaler, H. K. 1987. Chlorophylls and Carotenoids: Pigments of Photosynthetic Biomembranes. pp. 350–382 *in* L. Packer and R. Douce, editors. Methods in Enzymology. Academic Press, Inc.

Mayer, M., Chianese, R., Scudder, T., White, J., Vongpaseuth, K., and Ward, R. 2002. Thirteen Years of Monitoring the Hemlock Woolly Adelgid in New Jersey Forests. pp. 50–60 Hemlock Woolly Adelgid in the Eastern United States Symposium.

McClure, M. S. 1987. Biology and Control of Hemlock Woolly Adelgid, Bulletin 851. New Haven, CT.

McClure, M. S., and Cheah, C. A. S.-J. 1999. Reshaping the ecology of invading populations of hemlock woolly adelgid , Adelges tsugae (Homoptera : Adelgidae), in eastern North America. Biol. Invasions(1): 247–254.

Miller-Pierce, M. R., Orwig, D. A., and Preisser, E. 2010. Effects of hemlock woolly adelgid and elongate hemlock scale on eastern hemlock growth and foliar chemistry. Environ. Entomol. **39**(2): 513–9. doi:10.1603/EN09298.

Minocha, R., Martinez, G., Lyons, B., and Long, S. 2009. Development of a standardized methodology for quantifying total chlorophyll and carotenoids from foliage of hardwood and conifer tree species. Can. J. For. Res. **39**(4): 849–861. doi:10.1139/X09-015.

Orwig, D. A., and Foster, D. R. 1998. Forest Response to the Introduced Hemlock Woolly Adelgid in Southern New England, USA. J. Torrey Bot. Soc. **125**(1): 60–73.

Orwig, D. A., Thompson, J. R., Povak, N. A., Manner, M., Niebyl, D., and Foster, D. R. 2012. A foundation tree at the precipice : Tsuga canadensis health after the arrival of Adelges tsugae in central New England. Ecoshpere **3**(1): 1–16.

Oten, K. L. F., Cohen, A. C., and Hain, F. P. 2014. Stylet Bundle Morphology and Trophically Related Enzymes of the Hemlock Woolly Adelgid (Hemiptera: Adelgidae). Ann. Entomol. Soc. Am. **107**(3): 680–690.

Perboni, A. T., Cassol, D., da Silva, F. S. P., Silva, D. M., and Bacarin, M. A. 2012. Chlorophyll a fluorescence study revealing effects of flooding in canola hybrids. Biologia (Bratisl). **67**(2): 338–346. doi:10.2478/s11756-012-0006-0.

Pezet, J., Elkinton, J., Gomez, S., McKenzie, E. A., Lavine, M., and Preisser, E. 2013. Hemlock Woolly Adelgid and Elongate Hemlock Scale Induce Changes in Foliar and Twig Volatiles of Eastern Hemlock. J. Chem. Ecol. doi:10.1007/s10886-013-0300-5.

Pontius, J. A., Hallett, R. A., and Jenkins, J. C. 2006. Foliar Chemistry Linked to Infestation and Susceptibility to Hemlock Woolly Adelgid (Homoptera: Adelgidae). Environ. Entomol. **35**(1): 112–120. doi:10.1603/0046-225X-35.1.112.

Pontius, J., Hallett, R., and Martin, M. 2005a. Assessing hemlock decline using visible and near-infrared spectroscopy: indices comparison and algorithm development. Appl. Spectrosc. **59**(6): 836–43. doi:10.1366/0003702054280595.

Pontius, J., Hallett, R., and Martin, M. 2005b. Using AVIRIS to assess hemlock abundance and early decline in the Catskills, New York. Remote Sens. Environ. **97**(2): 163–173. doi:10.1016/j.rse.2005.04.011.

Radville, L., Chaves, A., and Preisser, E. L. 2011. Variation in plant defense against invasive herbivores: evidence for a hypersensitive response in eastern hemlocks (Tsuga canadensis). J. Chem. Ecol. **37**(6): 592–7. doi:10.1007/s10886-011-9962-z.

Rock, B. N., Hoshizaki, T., and Miller, J. R. 1988. Comparison of in situ and airborne spectral measurements of the blue shift associated with forest decline. Remote Sens. Environ. **24**(1): 109–127. doi:10.1016/0034-4257(88)90008-9.

Rock, B. N., Vogelmann, J. E., Williams, D. L., Vogelmann, A. F., and Hoshizaki, T. 1986. Remote detection of forest damage. Bioscience **36**(7): 439–445.

Rock, B. N., Williams, D. L., Moss, D. M., Lauten, G. N., and Kim, M. 1994. High-Spectral Resolution Field and Laboratory Optical Reflectance Measurements of Red Spruce and Eastern Hemlock Needles and Branches. Remote Sens. Environ. **47**: 176–189.

Rouse, J. W., Haas, R. H., Schell, J. A., and Deering, D. W. 1974. Monitoring Vegetation Systems in the Great Plains with ERTS. pp. 48–62 Proceedings of the 3rd Earth Resouce Technology Satellite Symposium.

Royle, D. D., and Lathrop, R. G. 2002. Discriminating Tsuga canadensis Hemlock Forest Defoliation using Remotely Sensed Change Detection. J. Nematol. **34**(3): 213–221.

Rubino, L., Charles, S., Sirulnik, A. G., Tuininga, A. R., and Lewis, J. D. 2015. Invasive insect effects on nitrogen cycling and host physiology are not tightly linked. Tree Physiol. **35**(2): 124–133. doi:10.1093/treephys/tpv004.

Strasser, R. J., Michael, M. T.-, and Srivastava, A. 2004. Analysis of the Fluorescence Transient. pp. 321–362 Chlorophyll a Fluorescence. Springer.

Strasser, R. J., Srivastava, A., and Tsimilli-Michael, M. 2000. The fluorescence transient as a tool to characterize and screen photosynthetic samples. pp. 443–480 Probing Photosynthesis: Mechanism, Regulation and Adaptation. Taylor and Francis, London.

Trotter, R. T., and Shields, K. S. 2009. Variation in winter survival of the invasive hemlock woolly adelgid (Hemiptera: Adelgidae) across the eastern United States. Environ. Entomol. **38**(3): 577–87.

Young, R. F., Shields, K. S., and Berlyn, G. P. 1995. Hemlock Woolly Adelgid (Homoptera: Adelgidae): Stylet Bundle Insertion and Feeding Sites. Ann. Entomol. Soc. Am.

Tables:

Table 1. Forest structure and percent basal area occupied by hemlock for each of the four study properties.

Site	Total Basal Area (m^2/ha)	Hemlock Basal Area (%)	Plot Density (stems/m^2)
Massabesic Exp. Forest	10 897.0	23.2	0.015
Northwood Meadows S.P.	16 297.0	46.2	0.033
Rachael Carson N.W.R.	5 552.2	18.3	0.010
Russell-Abbott State Forest	7 158.9	19.0	0.013

Table 2. A summary table of the number of infested and non-infested samples by site.

SITE	TREES SAMPLED	INFESTED	NON-INFESTED
Massabesic Exp. Forest	25	8	17
Northwood Meadows S.P.	23	23	0
Rachael Carson N.W.R.	24	3	21
Russell-Abbott State Forest	23	0	23

Table 3. A summary table of the number of significantly different narrow bands, within each spectral region, by sample month and growth year from the 2012 sampling period.

MONTH	GROWTH YEAR	VISIBLE 400-680 nm	RED EDGE 680-750 nm	NIR 750-1400 nm	MidIR 1400-2500 nm	TOTAL
JUNE	1	81	37	0	0	118
	2	0	0	0	0	0
JULY	1	57	1	0	4	62
	2	18	0	0	0	18
AUGUST	1	24	8	0	1	33
	2	9	1	0	0	10
SEPTEMBER	1	0	0	0	0	0
	2	1	0	0	1	2
OCTOBER	1	4	0	0	1	5
	2	1	0	0	0	1
NOVEMBER	1	27	0	0	1	28
	2	0	0	3	26	29
DECEMBER	1	0	0	0	2	2
	2	3	0	2	37	42

Table 4. *Z*-scores and corresponding *P*-values of Wilcoxon's Tests.

		REIP		NDVI		MSI		NIR 3/1	
MONTH	GROWTH YEAR	Z	Prob>|Z|	Z	Prob>|Z|	Z	Prob>|Z|	Z	Prob>|Z|
June	1	0.44771	0.6544	1.27775	0.2013	1.02220	0.3067	1.34312	0.1792
	2	-0.69499	0.4871	0.86796	0.3854	0.75290	0.4515	-0.28932	0.7723
July	1	0.19636	0.8443	0.84939	0.3957	-0.45736	0.6474	0.45695	0.6477
	2	-0.13067	0.8960	0.97919	0.3275	-2.15614	**0.0311***	-0.84863	0.3961
August	1	1.62938	0.1032	1.52075	0.1283	-1.03042	0.3028	-1.46428	0.1431
	2	-1.03270	0.3017	-0.16270	0.8708	-1.19400	0.2325	-2.22354	**0.0262***
September	1	1.85073	0.0642	1.19488	0.2321	-1.24735	0.2123	-1.46428	0.1431
	2	-0.16366	0.8700	-1.57856	0.1144	-0.86836	0.3852	-0.65127	0.5149
October	1	1.03985	0.2984	0.93741	0.3485	-2.46432	**0.0137***	-2.51620	**0.0119***
	2	0.14871	0.8818	-0.29587	0.7673	-2.16860	**0.0301***	-2.56422	**0.0103***
November	1	0.91472	0.3603	1.37578	0.1689	-2.41749	**0.0156***	-2.41749	**0.0156***
	2	-0.91884	0.3582	-1.24141	0.2145	-2.15421	**0.0312***	-2.41533	**0.0157***
December	1	2.09080	**0.0365***	0.00000	1.0000	0.00000	1.0000	0.12247	0.9025
	2	0.61237	0.5403	0.00000	1.0000	0.36742	0.7133	0.12247	0.9025

* Denotes statistically significant at α = 0.05

Table 5. A summary table of the number of significantly different narrow bands, within each spectral region, by sample month and growth year from the 2013 sampling period.

WEEK	VISIBLE 400-680 nm	RED EDGE 680-750 nm	NIR 750-1400 nm	MidIR 1400-2500 nm	TOTAL
4 June	0	0	3	3	6
10 June	3	0	0	2	5
17 June	1	0	28	1	30
24 June	0	0	0	0	0
1 July	44	12	0	4	60

Table 6. Statistical test and associated *P*-values for the 2013 spectral health indices data.

	REIP		NDVI		MSI		NIR 3/1	
DATE	Z	Prob>|Z|	Z	Prob>|Z|	Z	Prob>|Z|	Z	Prob>|Z|
04/16/2013	0.67316	0.5008	2.29783	**0.0216***	-0.83557	0.4034	-0.00000	1.0000
10/06/2013	1.18159	0.2374	0.62668	0.5309	-1.04447	0.2963	-0.21017	0.8335
17/06/2013	1.58114	0.1138	1.47120	0.1412	-0.83557	0.4034	-0.52382	0.6004
24/06//2013	0.40988	0.6819	1.35554	0.1752	-0.96825	0.3329	-0.58621	0.5577
01/07/2013	2.44718	**0.0144***	2.30482	**0.0212***	-1.36194	0.1732	-0.62668	0.5309

* Denotes statistically significant at α = 0.05

Table 7. Results of Wilcoxon's Test on pigment concentration in infested vs. non-infested hemlock foliage.

		CHL a		CHL b		CHLtot		CAR	
MONTH	GROWTH YEAR	Z	Prob>|Z|	Z	Prob>|Z|	Z	Prob>|Z|	Z	Prob>|Z|
June	1	0.894427	0.3711	0.638877	0.5229	0.894427	0.3711	-0.127775	0.8983
	2	-0.520774	0.6025	-0.636501	0.5244	-0.520774	0.6025	-0.636501	0.5244
July	1	0.979187	0.3275	0.326396	0.7441	0.979187	0.3275	0.718070	0.4727
	2	-0.326396	0.7441	-0.065279	0.9480	-0.065279	0.9480	-0.326396	0.7441
August	1	-1.620185	0.1052	-1.620185	0.1052	-1.620185	0.1052	-1.620185	0.1052
	2	-0.694365	0.4875	0.000000	1.0000	-0.694365	0.4875	0.694365	0.4875

* Denotes statistically significant at α = 0.05

Table 8. Results of Wilcoxon's Test on the 2013 extraction data.

	CHLa		CHL b		CHLtot		CARtot	
DATE	Z	Prob>|Z|	Z	Prob>|Z|	Z	Prob>|Z|	Z	Prob>|Z|
04/06/2013	2.078805	**0.0376***	1.322876	0.1859	1.927619	0.0539	2.759141	**0.0058***
10/06/2013	-0.037796	0.9698	0.264575	0.7913	0.037796	0.9698	0.264575	0.7913
17/06/2013	1.700840	0.0890	2.003212	**0.0452***	1.776433	0.0757	-0.113389	0.9097
24/06/2013	1.626346	0.1039	0.000000	1.0000	1.060660	0.2888	2.050610	**0.0403***
01/07/2013	2.305583	**0.0211***	0.000000	1.0000	1.776433	0.0757	-0.642540	0.5205

* Denotes statistically significant at α = 0.05

Table 9. Results of Wilcoxon's Test on fluorescence parameters.

	Fv/Fm		PIabs		PItot	
DATE	Z	Prob>|Z|	Z	Prob>|Z|	Z	Prob>|Z|
04/06/2013	0.908251	0.3637	1.960676	**0.0499***	2.373321	**0.0176***
10/06/2013	0.430132	0.6671	-1.220062	0.2224	-2.750000	**0.0060***
17/06/2013	-0.407646	0.6835	0.523877	0.6004	1.338797	0.1806
24/06/2013	0.635869	0.5249	2.569209	**0.0102***	2.915619	**0.0035***
01/07/2013	-0.400880	0.6885	-3.790000	**0.0002***	-4.990000	**<.0001***

* Denotes statistically significant at α = 0.05

Figure Captions:

Fig. 1. A map of the region of indicating the locations of the study plots.

Fig. 2. Reflectance difference as measured in percent (left column), and sensitivity curves (right column), of first year foliage from June through December of 2012. Negative difference (%) values indicated wavelengths at which infested foliage exhibited lesser reflectance than non-infested foliage. Sensitivity curves highlight the reflectance wavelengths at which a response to HWA infestation may be detected. Vertical lines at 680 nm, 750 nm, and 1400 nm denote the visible, red edge, NIR and MidIR spectral regions.

Fig. 3. Graphs indicating the spectral bands that were statistically significant when comparing infested and non-infested foliage from the 2012 sampling period. The graphs are arranged by month in rows, and by growth year in columns. Statistical significance is denoted by black markers below the 0.05 significance level line. Only p-values below 0.20 are shown. Vertical lines at 680 nm, 750 nm, and 1400 nm denote the visible, red edge, NIR and MidIR spectral regions.

Fig. 4. Reflectance difference as measured in percent (left column), and sensitivity curves (right column), of second year foliage from June through December of 2012. Vertical lines at 680 nm, 750 nm, and 1400 nm denote the visible, red edge, NIR and MidIR spectral regions.

Fig. 5. Outlier box plots of spectral health indices data for first year (left column) and second year (right column) growth by month in 2012 for infested and non-infested foliage. Asterisks indicate statistically significant differences ($\alpha = 0.05$) between infested and non-infested foliage. Sample size values for each month are noted in Figures 2 and 4.

Fig. 6. First year foliage reflectance difference as measured in percent (left column), and sensitivity curves (right column), from the 2013 Massabesic Experimental Forest data collection.

Vertical lines at 680 nm, 750 nm, and 1400 nm denote the visible, red edge, NIR and MidIR spectral regions.

Fig. 7. Graphs indicating the spectral bands that were statistically significant when comparing infested and non-infested foliage from the 2013 sampling period. Statistical significance is denoted by black markers below the 0.05 significance level line. Only p-values below 0.20 are shown. Vertical lines at 680 nm, 750 nm, and 1400 nm denote the visible, red edge, NIR and MidIR spectral regions.

Fig. 8. Outlier box plots of spectral health indices data from the 2013 Massabesic Experimental Forest first year foliage. Asterisks indicate statistically significant ($\alpha = 0.05$) differences between infested and non-infested foliage. Sample size values for each week are noted in Figure 6.

Fig. 9. Chlorophyll data from the 2013 Massabesic Experimental Forest data collection comparing non-infested (dark grey) and HWA infested (light grey) hemlock foliage for first year growth. Asterisks indicate statistical differences ($\alpha = 0.05$) between infested and non-infested foliage for that week. For each week infested and non-infested groups $n = 5$, except for 24 June infested foliage when $n = 3$.

Fig. 10. Fluorescence parameter data indicating that infested foliage absorbed greater photon energy and had a greater photosynthetic performance index value. Asterisks indicate statistically significant ($\alpha = 0.05$) differences between infested and non-infested foliage.

Fig. 11A. Outlier box plots of weekly foliar moisture content values from the 2013 Massabesic Experimental Forest data collection. **11B**. Correlation of the MSI to foliar moisture content values, indicating that as foliar moisture content decreased MSI values increased.

Fig. 1

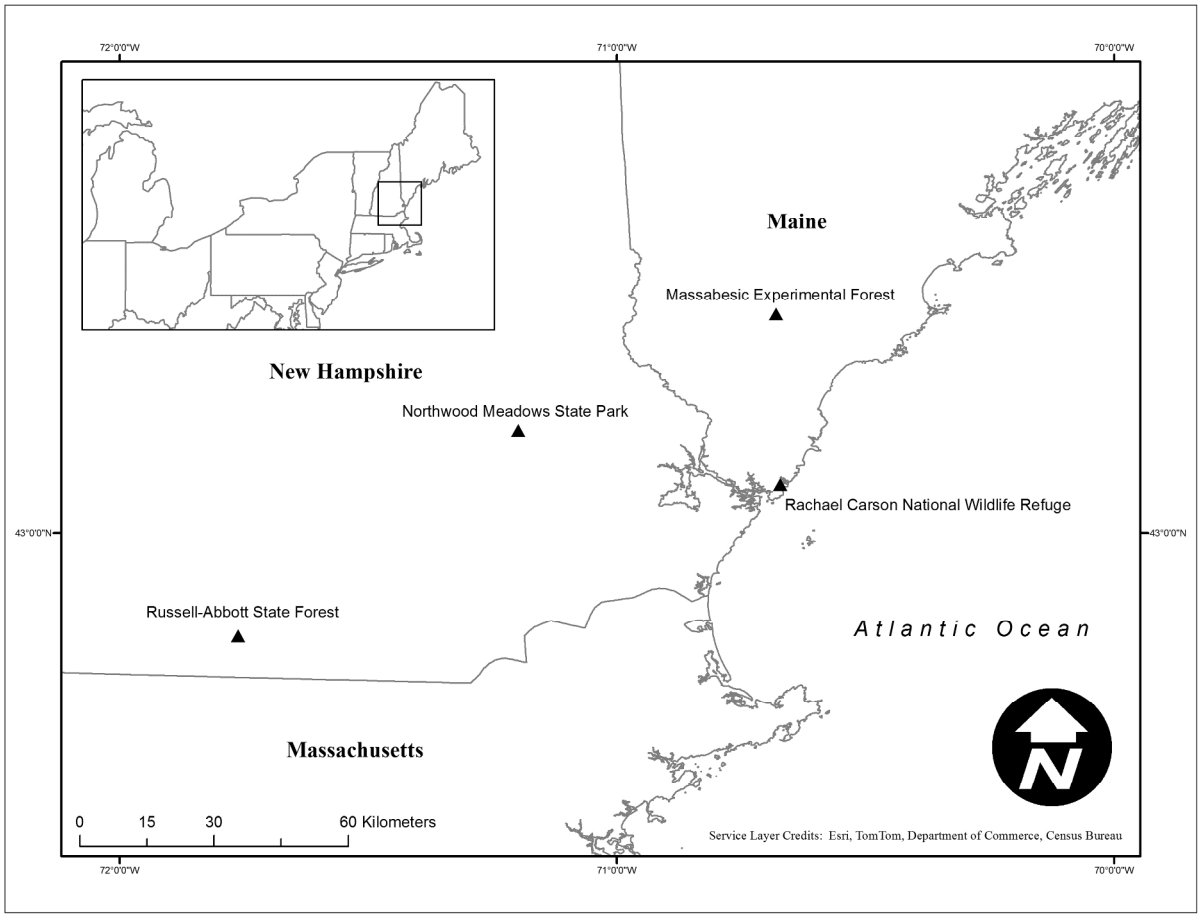
72°0'0"W
71°0'0"W
70°0'0"W
Maine
Massabesic Experimental Forest
New Hampshire
Northwood Meadows State Park
Rachael Carson National Wildlife Refuge
43°0'0"N
Russell-Abbott State Forest
Atlantic Ocean
Massachusetts
N
0 15 30 60 Kilometers
Service Layer Credits: Esri, TomTom, Department of Commerce, Census Bureau

Fig. 2

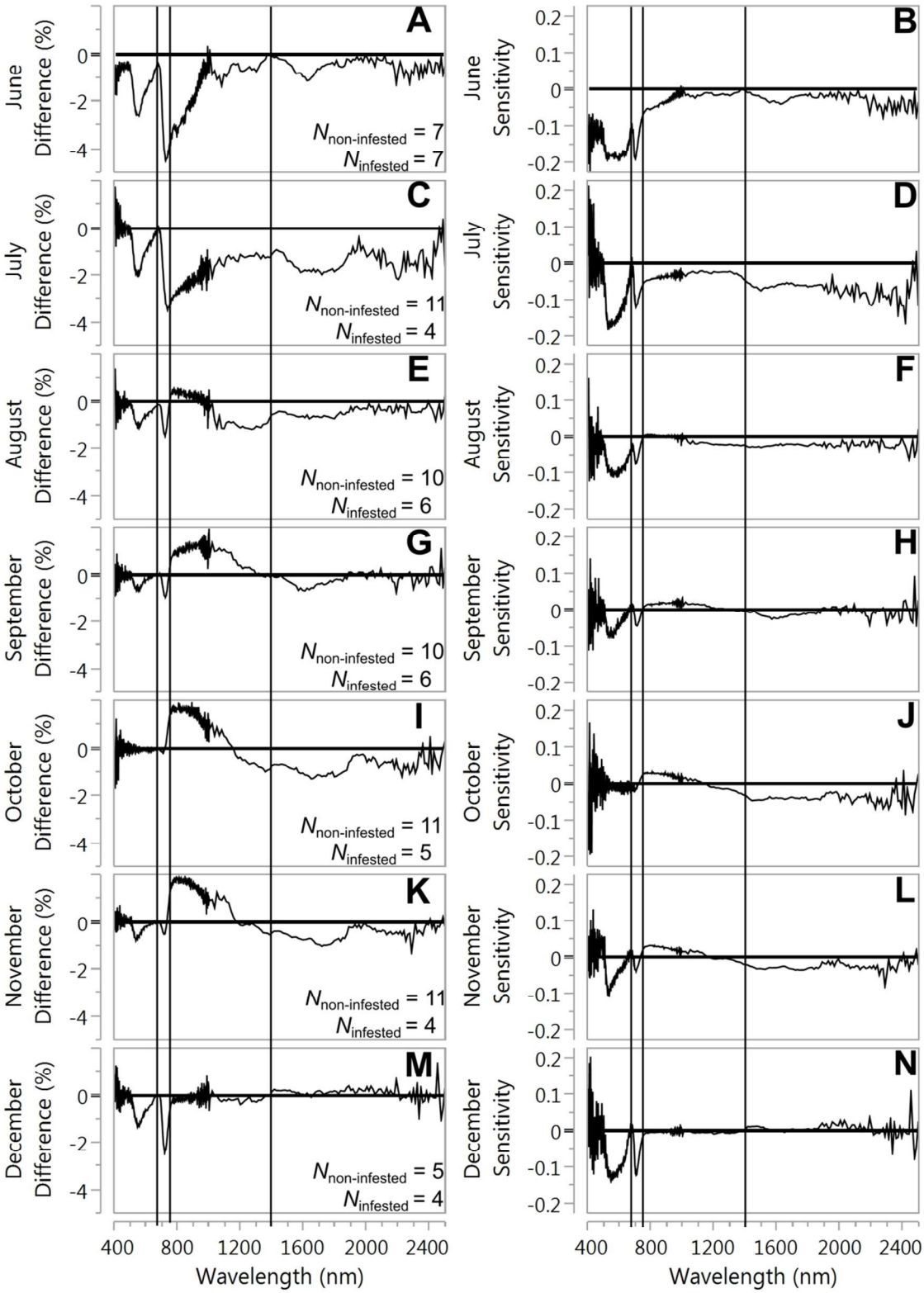
A
B
C
D
E
F
G
H
I
J
K
L
M
N
June Difference (%)
June Sensitivity
July Difference (%)
July Sensitivity
August Difference (%)
August Sensitivity
September Difference (%)
September Sensitivity
October Difference (%)
October Sensitivity
November Difference (%)
November Sensitivity
December Difference (%)
December Sensitivity
$N_{non\text{-}infested}$ = 7
$N_{infested}$ = 7
$N_{non\text{-}infested}$ = 11
$N_{infested}$ = 4
$N_{non\text{-}infested}$ = 10
$N_{infested}$ = 6
$N_{non\text{-}infested}$ = 10
$N_{infested}$ = 6
$N_{non\text{-}infested}$ = 11
$N_{infested}$ = 5
$N_{non\text{-}infested}$ = 11
$N_{infested}$ = 4
$N_{non\text{-}infested}$ = 5
$N_{infested}$ = 4
0
-2
-4
0.2
0.1
-0.1
-0.2
400
800
1200
1600
2000
2400
Wavelength (nm)

Fig. 3

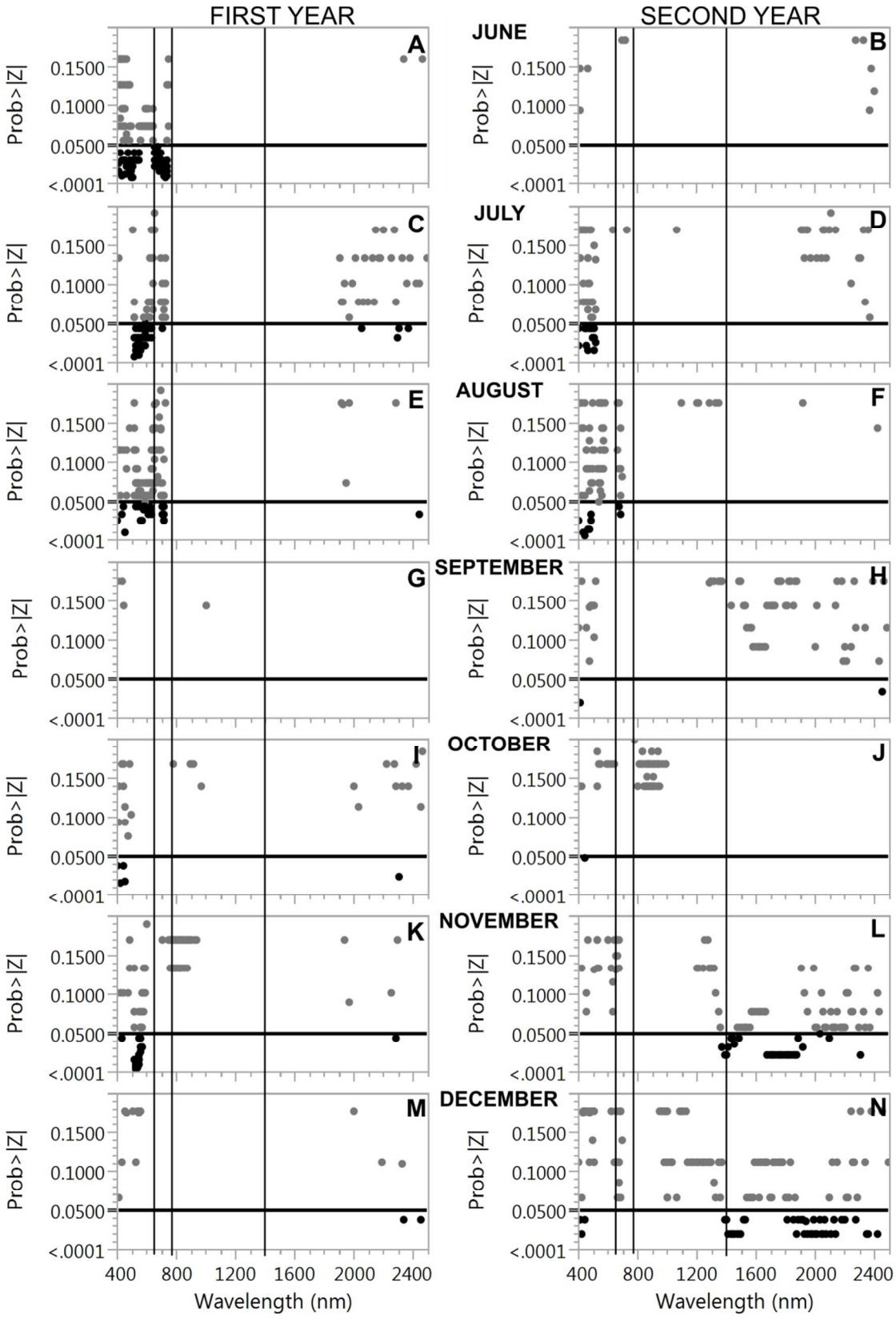
FIRST YEAR
SECOND YEAR
JUNE
JULY
AUGUST
SEPTEMBER
OCTOBER
NOVEMBER
DECEMBER
A
B
C
D
E
F
G
H
I
J
K
L
M
N
Prob>|Z|
0.1500
0.1000
0.0500
<.0001
400
800
1200
1600
2000
2400
Wavelength (nm)

Fig. 4

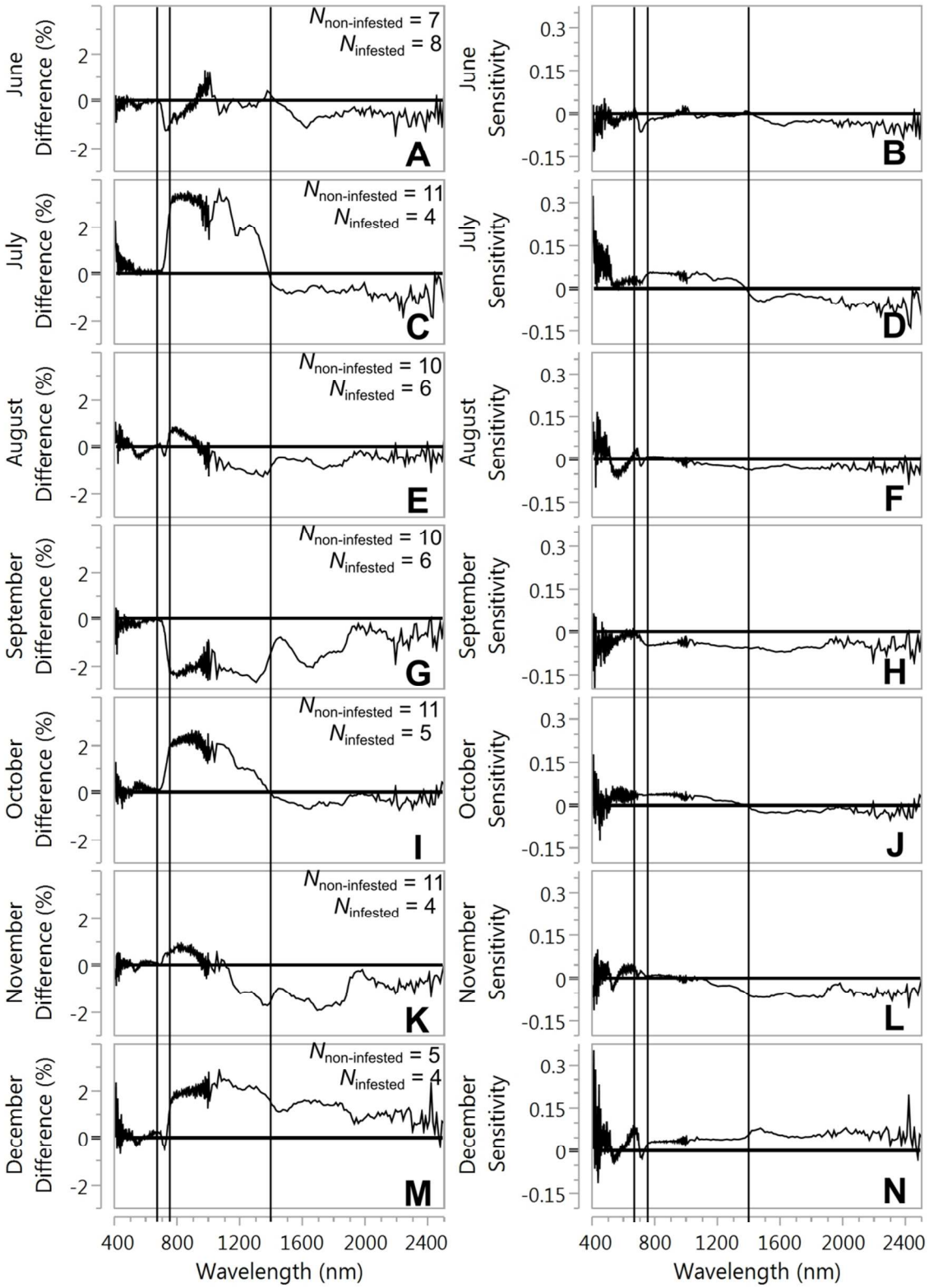
June Difference (%)
$N_{non-infested}$ = 7
$N_{infested}$ = 8
A
June Sensitivity
B
July Difference (%)
$N_{non-infested}$ = 11
$N_{infested}$ = 4
C
July Sensitivity
D
August Difference (%)
$N_{non-infested}$ = 10
$N_{infested}$ = 6
E
August Sensitivity
F
September Difference (%)
$N_{non-infested}$ = 10
$N_{infested}$ = 6
G
September Sensitivity
H
October Difference (%)
$N_{non-infested}$ = 11
$N_{infested}$ = 5
I
October Sensitivity
J
November Difference (%)
$N_{non-infested}$ = 11
$N_{infested}$ = 4
K
November Sensitivity
L
December Difference (%)
$N_{non-infested}$ = 5
$N_{infested}$ = 4
M
December Sensitivity
N
2
0
-2
0.3
0.15
0
-0.15
400 800 1200 1600 2000 2400
Wavelength (nm)

Fig. 5

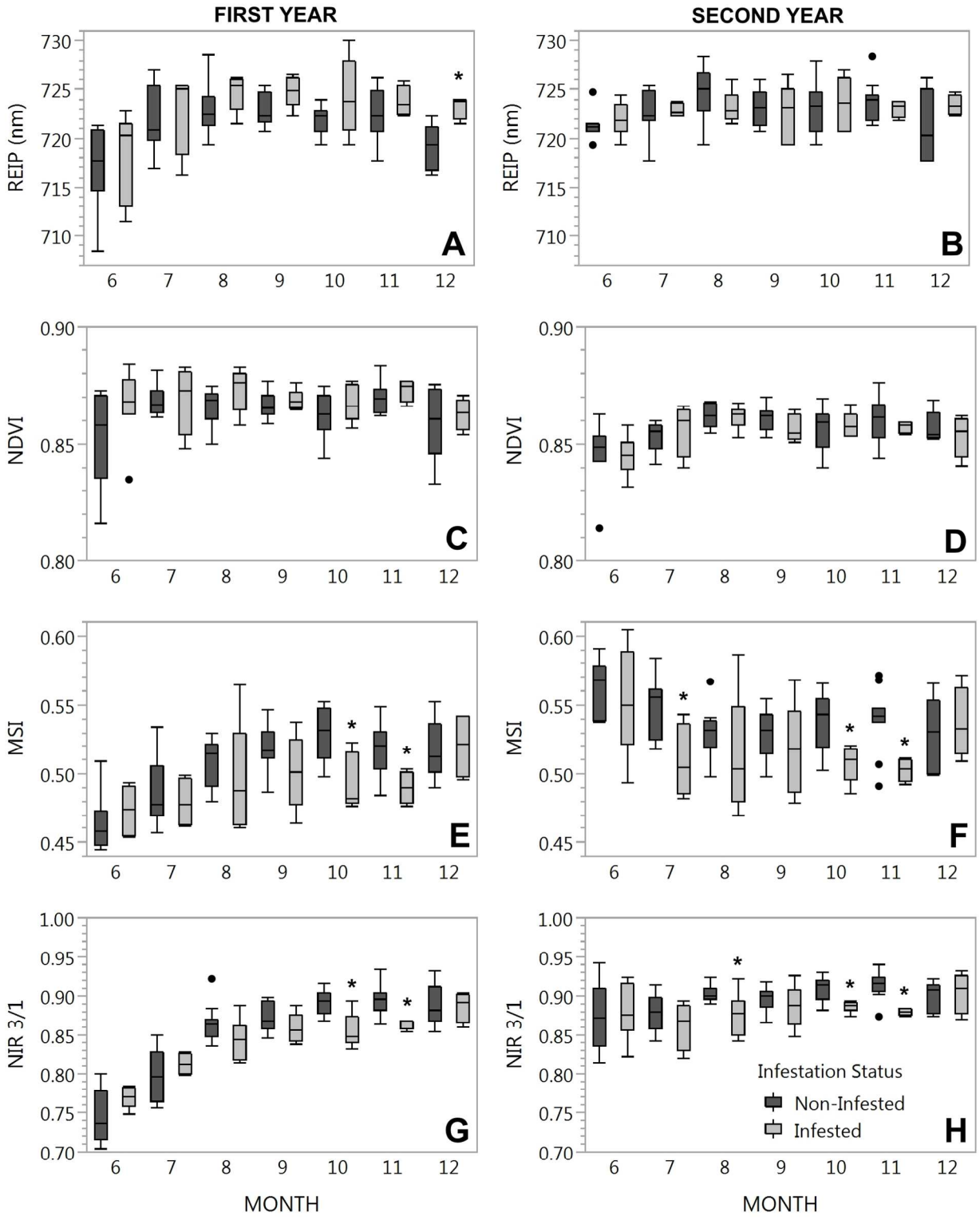
FIRST YEAR
SECOND YEAR
REIP (nm)
NDVI
MSI
NIR 3/1
MONTH
A
B
C
D
E
F
G
H
Infestation Status
Non-Infested
Infested

Fig. 6

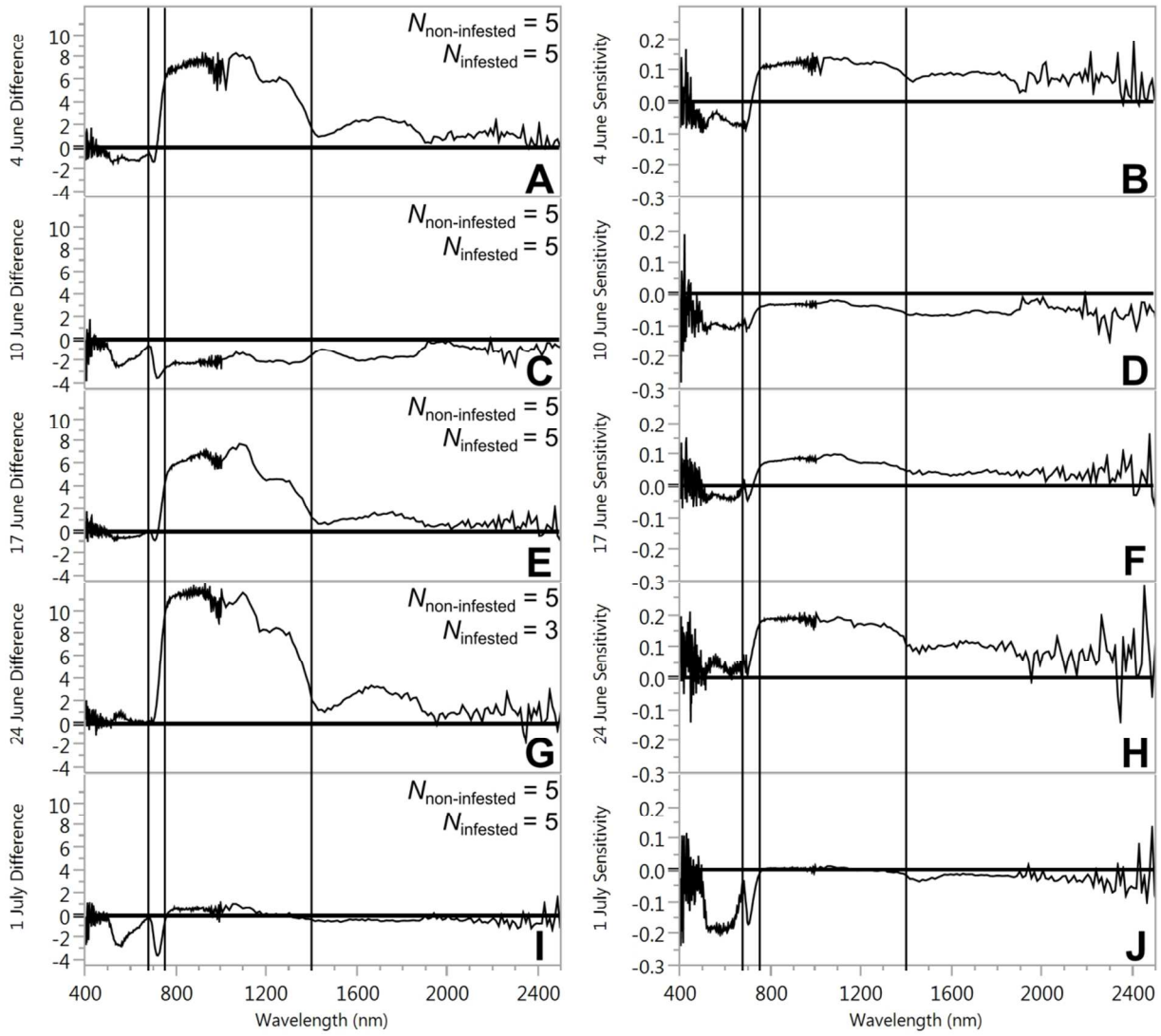
4 June Difference
10 June Difference
17 June Difference
24 June Difference
1 July Difference
4 June Sensitivity
10 June Sensitivity
17 June Sensitivity
24 June Sensitivity
1 July Sensitivity
$N_{non-infested}$ = 5
$N_{infested}$ = 5
$N_{infested}$ = 3
A
B
C
D
E
F
G
H
I
J
Wavelength (nm)

Fig. 7

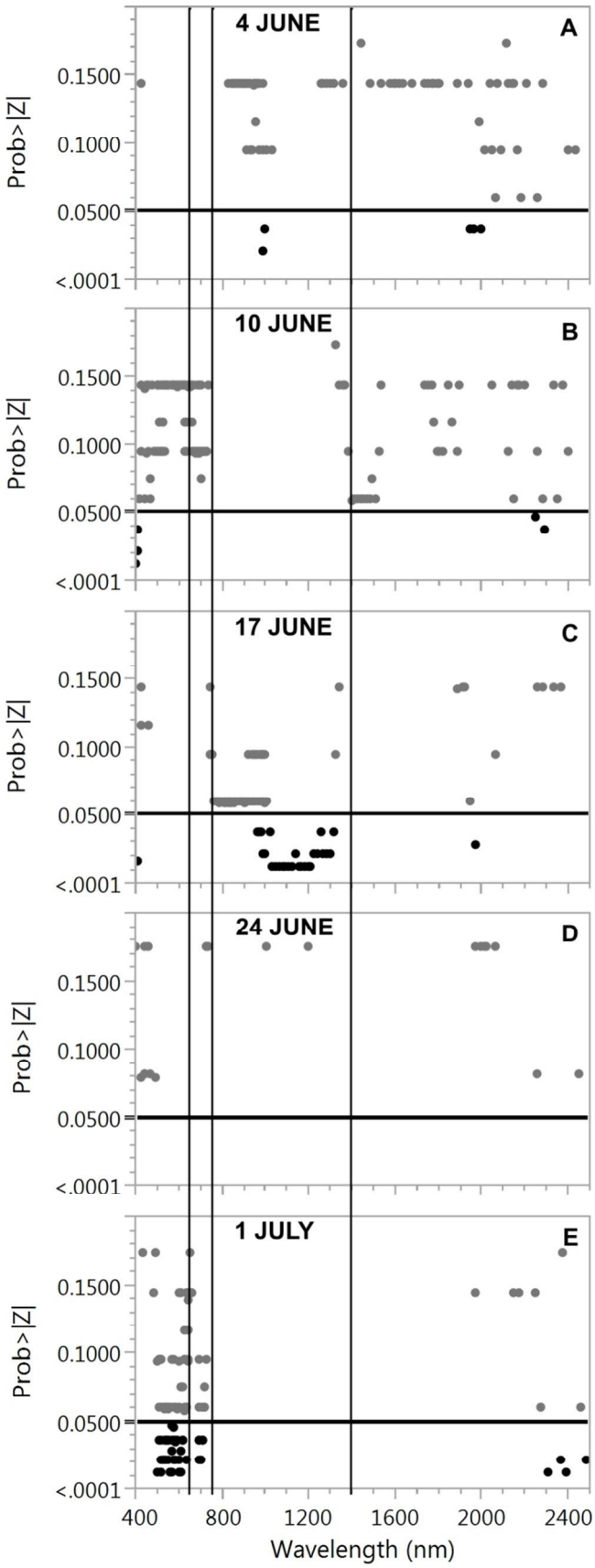
4 JUNE
A
10 JUNE
B
17 JUNE
C
24 JUNE
D
1 JULY
E
Prob>|Z|
0.1500
0.1000
0.0500
<.0001
400
800
1200
1600
2000
2400
Wavelength (nm)

Fig. 8

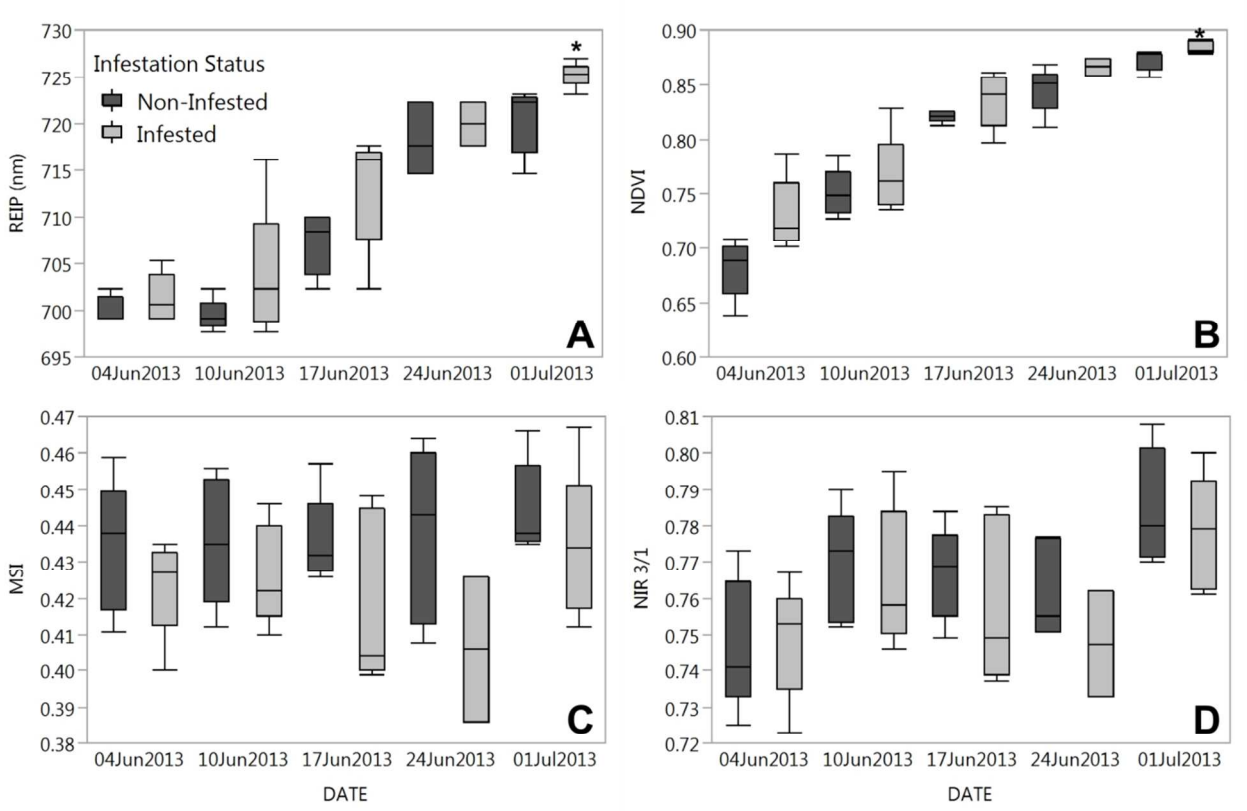
Infestation Status
Non-Infested
Infested
REIP (nm)
NDVI
MSI
NIR 3/1
A
B
C
D
04Jun2013
10Jun2013
17Jun2013
24Jun2013
01Jul2013
DATE

Fig. 9

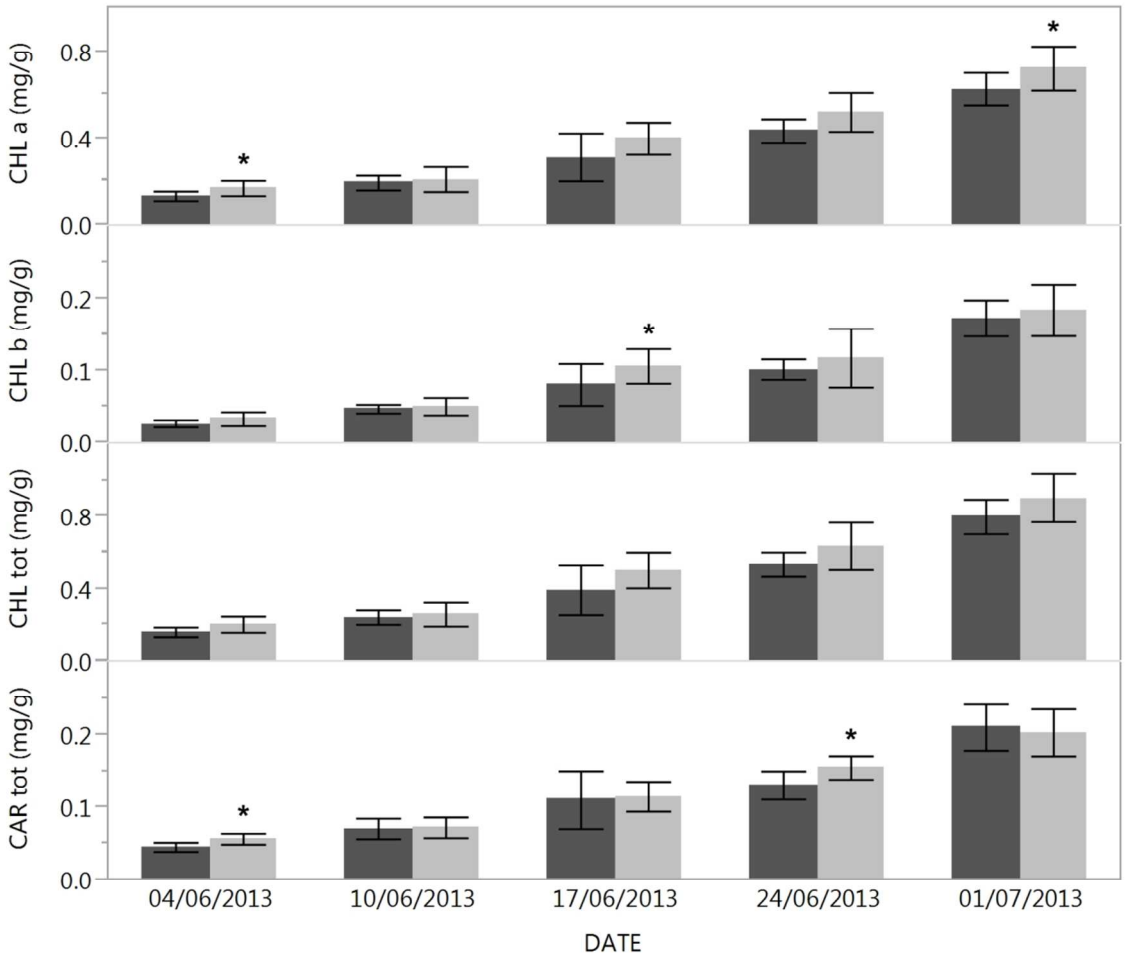
CHL a (mg/g)
CHL b (mg/g)
CHL tot (mg/g)
CAR tot (mg/g)
0.0
0.1
0.2
0.4
0.8
*
04/06/2013
10/06/2013
17/06/2013
24/06/2013
01/07/2013
DATE

Fig. 10

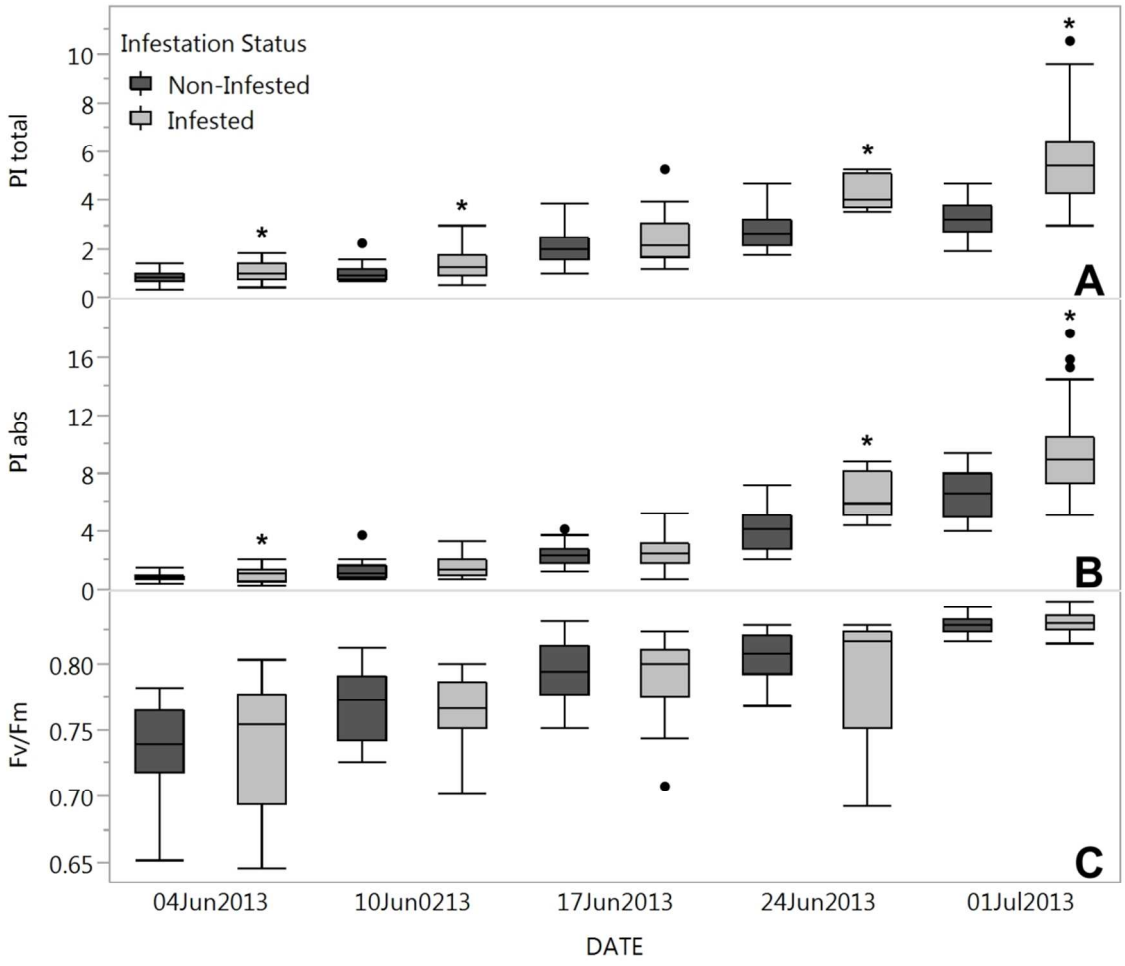
Infestation Status
Non-Infested
Infested
PI total
PI abs
Fv/Fm
A
B
C
04Jun2013
10Jun0213
17Jun2013
24Jun2013
01Jul2013
DATE

Fig. 11

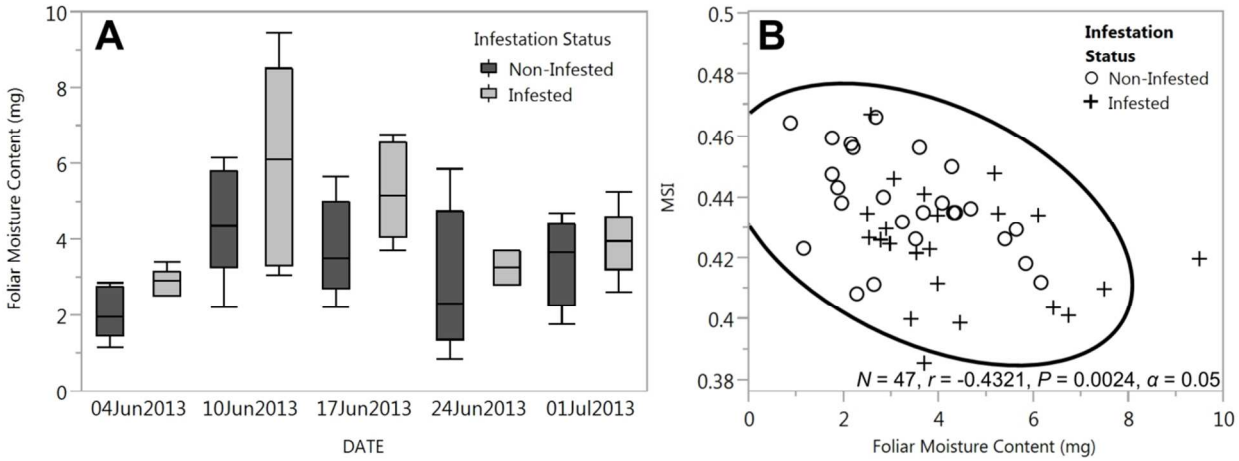
A
Infestation Status
Non-Infested
Infested
Foliar Moisture Content (mg)
DATE
04Jun2013
10Jun2013
17Jun2013
24Jun2013
01Jul2013
B
Infestation Status
Non-Infested
Infested
MSI
Foliar Moisture Content (mg)
N = 47, r = -0.4321, P = 0.0024, α = 0.05